MEASUREMENT OF SURFACE TENSION IN BASE METAL SULFIDE MATTES BY AN IMPROVED SESSILE DROP METHOD

by

Joseph Hamuyuni

Thesis presented in partial fulfilment
of the requirements for the degree

of

Master of Science in Engineering
(Extractive Metallurgical Engineering)

in the Faculty of Engineering
at Stellenbosch University

Supervisor

Prof. G. Akdogan

Co-Supervisors

Prof. S.M. Bradshaw
Prof. P. Taskinen (Aalto University)

December 2012

DECLARATION

By submitting this thesis electronically, I declare that the entirety of the work contained therein is my own, original work, that I am the sole author thereof (save to the extent explicitly otherwise stated), that reproduction and publication thereof by Stellenbosch University will not infringe any third party rights and that I have not previously in its entirety or in part submitted it for obtaining any qualification.

Joseph Hamuyuni

Signature: Date: 15/11/2012

ABSTRACT

Smelting of sulfide concentrate is an important process stage in the metal making industry, especially in copper and nickel processes where concentrates must be smelted and often converted to produce an impure metal suitable for electrorefining. Smelting is a complex process and is sometimes difficult to control because of the high working temperatures involved and the complexity of phases present at these conditions. At the bottom of the smelting furnace is the settling zone, where molten sulfides (matte) and impurity phase (slag) collect. The low density slag settles on top of the matte and is often intermittently tapped.

One of the major dilemmas of the smelting furnace is the mechanical loss of metal to the slag. This is largely influenced by flotation of metal droplets in the slag phase. Depending on the operating conditions, gas bubbles entering the slag phase may float the dispersed droplets away from the matte-slag interface. The ability of gas bubbles to pick up matte droplets is governed by properties such as surface tension, viscosity and density of the molten matte and slag. Interactions of matte and slag at the slag-matte interface by the Marangoni effect also lead to rapid corrosion of refractories. Therefore, in order to predict phase behaviour, physical properties such as surface tension, viscosity, and density are quantified. Values of matte surface tension are vital to understanding the gas-slag-matte phenomena in smelting operations.

A sessile drop apparatus has been developed to measure the surface tension for selected mattes, resting on an alumina substrate. In the apparatus, modifications have been done to the optical system to improve the accuracy.

Specifically, surface tensions of pure Ni_3S_2, Cu_2S and FeS molten phases were measured using an improved sessile drop method in an inert atmosphere of purified argon, as a function of temperature and composition (at 1200 ^{o}C). The surface tension values were obtained over a temperature range from 1000 to 1300 ^{o}C. In this temperature range, surface tension of molten Ni_3S_2 decreased linearly with increasing temperature. However, the surface tensions of molten FeS and Cu_2S phases were approximately

constant over this range of temperature. The pseudo-binary and ternary system results indicated that surface tension is greatly influenced by Ni_3S_2, and FeS, and that the addition of Cu_2S to this system has only a limited effect on surface tensions. Measured values are compared with experimental values in literature and found to differ to a maximum of 5.91 % over all compositions and temperatures investigated

The sessile drop method can therefore be used to measure surface tension of molten mattes.

OPSOMMING

Die smelting van sulfiedkonsentraat is ’n belangrike prosesstadium in die metaalvervaardigingsbedryf, veral in koper- en nikkelprosesse waar konsentrate gesmelt en dikwels ook gesementeer moet word om ’n onsuiwer metaal te skep wat vir elektroaffinering geskik is. Smelting is ’n komplekse proses, en is soms moeilik om te beheer weens die hoë werkstemperature en die kompleksiteit van die fases wat in hierdie toestande aanwesig is. Onder in die smeltoond is die neerslagsone, waar gesmelte sulfiede (swawelmetaal) en onsuiwerheidsfase (slak) versamel. Die slak, wat oor ’n lae digtheid beskik, gaan lê bo-op die swawelmetaal, en word gewoonlik met tussenposes afgetap.

Een van die groot dilemmas van die smeltoond is die meganiese verlies van metaal wat in die slak beland. Dit word grootliks beïnvloed deur die flottasie van metaaldruppels in die slakfase. Na gelang van die werkstoestande kan gasborrels wat die slakfase binnegaan die gedispergeerde druppels wegdryf van die swawelmetaal-slak-tussenvlak. Die vermoë van die gasborrels om swawelmetaaldruppels op te tel word bepaal deur eienskappe soos die oppervlakspanning, viskositeit en digtheid van die gesmelte swawelmetaal en slak. Die wisselwerking tussen swawelmetaal en slak as gevolg van die Marangoni-effek op die tussenvlak van dié twee komponente lei ook tot die snelle korrosie van vuurvaste materiaal. Om dus fasegedrag te voorspel, word fisiese eienskappe soos oppervlakspanning, viskositeit en digtheid gekwantifiseer. Die oppervlakspanningswaardes van die swawelmetaal is noodsaaklik om die gas-slak-swawelmetaal-verskynsel in smeltbewerkings te verstaan.

’n Sessiele drupapparaat is ontwikkel om vanaf ’n aluminasubstraat die oppervlakspanning vir bepaalde swawelmetale te bepaal. Sekere veranderinge is aan die optiese stelsel in die apparaat aangebring om akkuraatheid te verbeter.

In die besonder is die oppervlakspanning van suiwer Ni_3S_2-, Cu_2S- en FeS-gesmelte fases met behulp van ’n verbeterde sessiele drupmetode in ’n trae

atmosfeer van gesuiwerde argon gemeet as ’n funksie van temperatuur en samestelling (teen 1 200 °C). Die oppervlakspanningswaardes is oor ’n temperatuurbestek van 1 000–1 300 °C verkry. In hierdie bestek het die oppervlakspanning van gesmelte Ni_3S_2 lineêr afgeneem namate temperatuur gestyg het. Tog was die oppervlakspannings van die gesmelte FeS - en Cu_2S -fases min of meer konstant oor hierdie temperatuurbestek. Die pseudobinêre en -ternêre stelselresultate dui daarop dat oppervlakspanning beduidend beïnvloed word deur Ni_3S_2 en FeS , en dat die byvoeging van Cu_2S by hierdie stelsel slegs ’n beperkte uitwerking op oppervlakspanning het. Die gemete waardes is met proefwaardes in die literatuur vergelyk en het oor alle bestudeerde samestellings en temperature heen met hoogstens 5,91% verskil.

Die sessiele drupmetode kan dus gebruik word om die oppervlakspanning van gesmelte swawelmetaal te meet.

ACKNOWLEDGEMENTS

Firstly I would like to thank God for his unfailing love and provisions throughout this study.

I am heartily thankful to my supervisors, Prof G. Akdogan and Prof S.M. Bradshaw, for encouragement, guidance and support towards the successful completion of this study. This enabled me to develop a thorough understanding of the subject.

I specially thank Prof. Pekka Taskinen (Head of Thermodynamics and Modeling Research group of Aalto University) for such a great opportunity, for his supervision and for providing an enabling environment during this work.

Table of Contents

List of Figures

List of Tables

NOMENCLATURE

Alphabetical Symbols

a_i	Activity of gas	
c	Concentration of the surface active component	[M.L^{-1}]
g	Acceleration due to gravity	[m.s^{-2}]
h	Infiltration height	[m]
P_i	Partial pressure of a gas	[atm]
P^{Θ}	Standard pressure	[atm]
r	The radius of a capillary	[m]
r_{drop}	Diameter of a metal drop	[m]
R_1; R_2	The principal radii of curvature of the surface	[m]
S	Area	[m^2]
T	Temperature	[^{o}C]

Greek Symbols

β	Shape factor	
γ	Surface/interfacial tension	[N.m^{-1}]
$\gamma_{m/g}$	Matte surface tension	[N.m^{-1}]
$\gamma_{m/s}$	Matte-slag surface tension	[N.m^{-1}]
$\gamma_{s/g}$	Slag surface tension	[N.m^{-1}]
Δ	Flotation coefficient	
Δp	Pressure gradient	
η	Literature surface tension values	[N.m^{-1}]

θ	Contact angle	[^{o}]
μ_{slag}	Slag viscosity	[g.cm^{-1}s^{-1}]
v	Settling velocity	[m.s^{-1}]
ρ_{drop}	Density of an enclosed metal particle	[kg.cm^{-3}]
ρ_{slag}	Density of slag	[kg.cm^{-3}]
σ	Standard Deviation of experimental results	
τ_s	Surface shear stress	[N.m^{-2}]
Φ	Spreading Coefficient	
φ	Electrical potential	

Commonly used Acronyms

CCD	Charge coupled device
CMOS	Complementary metal oxide semiconductor
FSF	Flash smelting Furnace
FTÅ	First ten angstroms
STDEV	Standard deviation of the results at each temperature

1 Introduction

1.1 The role of physical properties in pyrometallurgical processes

The first stage of extractive metallurgy involves size reduction of the ore to unlock the valuable mineral from its associated gangue at the coarsest particle size. Separation techniques such as flotation are then applied to obtain a concentrate with increased metal content (Davenport et al., 2002). For sulfide ores, the extraction stage often involves pyrometallurgical processes such as smelting, which subject these concentrates to suitable high temperatures where valuable metals can easily be recovered. Pyrometallurgy is the branch of extractive metallurgy that involves thermal treatment of ore and mineral concentrates to bring about physical and chemical transformations in the materials to enable recovery of valuable metals. The refining stage is for the purpose of removing impurities. This is illustrated in Figure 1.

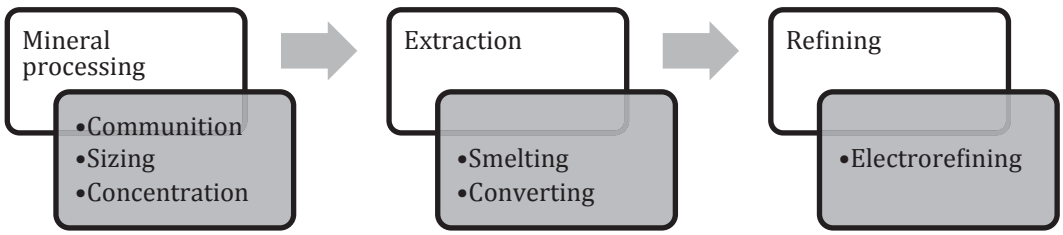

Figure 1: Extractive metallurgy processes.

The need for more efficient smelting processes to recover required metals at reduced energy levels has become very important to the pyrometallurgical industry (Davenport et al., 2002). In Copper (Cu) and Nickel (Ni) smelting processes, for example, this efficiency is to a great extent influenced by physicochemical properties of the molten phases (matte and slag) (Davenport et al., 2002; Kucharski et al., 1993). These properties include density, viscosity and surface tension. Physical properties of molten mattes

and slags in pyrometallurgy of Copper and Nickel are crucial in resultant phase phenomena, such as matte and slag separation and settling (Davenport et al., 2002; Ip and Toguri, 1993; Minto and Davenport, 1972).

1.2 Surface and interfacial phenomena

Surface properties of molten mattes and slags therefore also play a significant role in metal extraction from their sulfide concentrates. They also help understand matte entrainment in slag and slag-gas emulsions, as well as the corrosion of refractories caused by interactions of molten mattes and slag (Liukkonen, 1998; Carlos, 1974; Kucharski et al., 1993; Ip and Toguri, 1993). During the smelting of sulfides, surface active substances such as silica are often introduced into the matte-slag system. These substances reduce the surface tension of most oxides which collects on top as slag (Davenport, 2002). At the same time, the molten matte tends to coalesce as matte droplets under the action of surface and interface tension. This action contributes to the separation of matte and slag, but can cause corrosion of refractory lining at the interface due to interaction of matte and slag phases. Figures 2 and 3 depict matte slag interaction. Contact angles (Figure 3) are given as θ and φ at the matte–gas and matte–slag interfaces respectively.

Contact angle

The contact angle is defined as the angle created by a joint of the liquid-solid boundary with the liquid-air boundary. It is the angle between a solid specimens' surface and the tangent of the droplet's oval shape at droplet boundary (Eustathopoulos et al., 1999). A large contact angle describes low solid surface energy, a phenomenon also denoted as a low degree of wetting. On the other hand, a low contact angle describes a high solid surface energy. A contact angle of zero degrees describes complete wetting, and will occur if the droplet takes the shape of a flat puddle, see Figure 4 (Eustathopoulos et al., 1999).

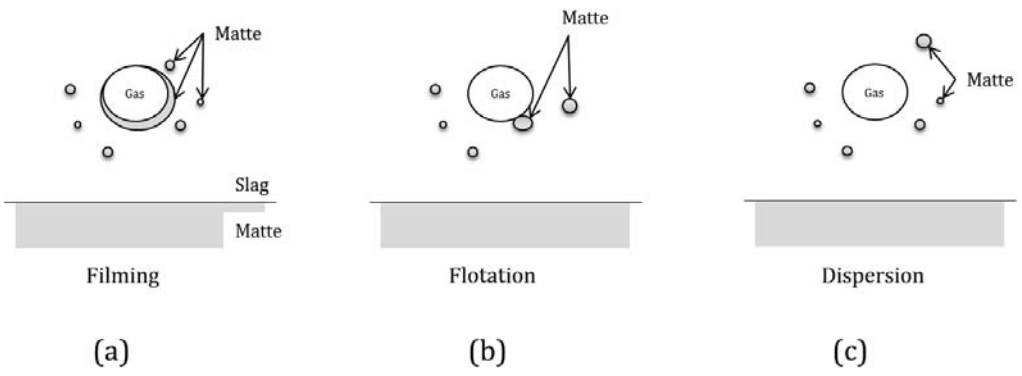

Figure 2: Gas bubble - liquid droplet interactions in continuous phase (a) Filming of droplets on gas bubble, (b) droplet attachement to bubble, (c) droplet dispersion, (adapted from Minto and Davenport, 1972).

At various atmospheric conditions of temperature and pressure, physical properties will influence phase separation i.e. the amount of metal that reports to matte as well as the matte droplets that can report mechanically to slag.

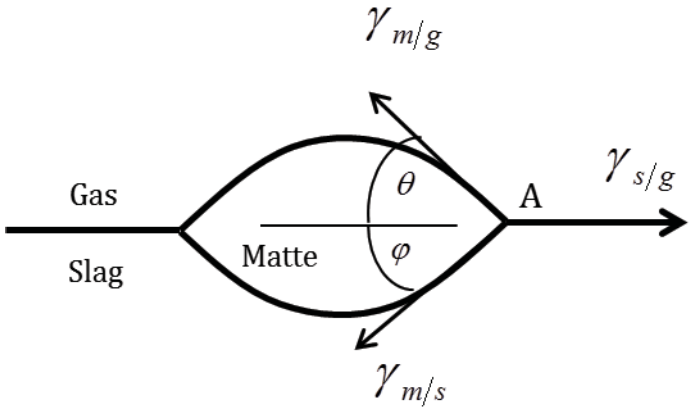

Figure 3: Conochie and Robertson's formulation of the droplet configuration (adapted from Ip and Toguri, 1992).

Main sources of mechanically transported matte through droplets in slag include: slag recycled from the converting process, metal contained in dispersed matte moving from matte phase towards the slag phase, metal that precipitates due to varied furnace temperature gradients, sulfur dioxide (gas bubbles) generated by the smelting reactions disperse metal in form of droplets to slag, matte can also attach to magnetite slag species which slows the rate at which drops settles. (Ip and Toguri, 1992; Minto and

Davenport,1972). The mechanical loss of matte to slag alone accounts for ~70 % of the total loss for smelters with no slag cleaning stage (Davenport et al, 2002).

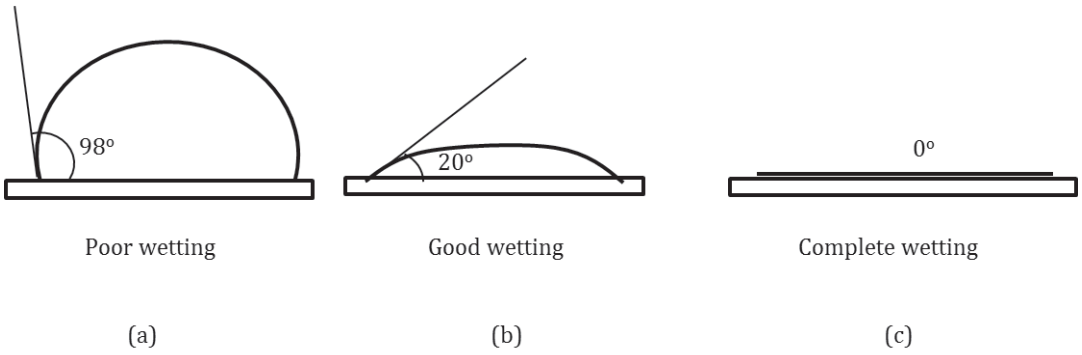

Figure 4: schematic of the three possible degrees of wetting with corresponding approximate contact angles (adapted from Eustathopoulos et al., 1999).

During smelting of base metal sulfide concentrates, matte and slag properties vary depending on different conditions of temperature, matte grade, oxygen partial pressure, and causing the matte-slag interactions to vary. For example, sulfur gas bubbles can either collect metal in form of droplets by attachement and floting them, or disperse the matte droplets. This behaviour is driven by surface tension and interfacial tension of matte – slag phase. (Minto and Davenport, 1999) proposed that filming in (a) will occur when the spreading coefficient (Equation 1) as defined by (Harkins and Jordan, 1930) is positive:

$$\Phi = \gamma_{s/g} - \gamma_{m/g} - \gamma_{m/s} \qquad \text{Equation 1}$$

Where $\gamma_{s/g}$ is the slag surface tension,

$\gamma_{m/g}$ is the matte surface tension, and

$\gamma_{m/s}$ the matte – slag interfacial tension.

(Minto and Davenport, 1999) also proposed that floting in (b) of matte droplets (b) in Figure 2 will occur when the flotation coefficient is greater than zero:

$$\Delta \approx \gamma_{s/g} - \gamma_{m/g} + \gamma_{m/s}$$ Equation 2

Case (c) (Figure 2) will take place if the flotation coefficient is less than zero.

Surface tensions of molten matte and slag phases therefore become an important parameter that should be clearly understood during the smelting process. (Davenport et al., 2002; Liukkonen, 1998; Kucharski et al., 1993; Tokumoto et al., 1972)

While much data on mattes has been obtained for density and viscosity at various temperature ranges, accurate surface tension data are scarce. This is due to the complexity of phases as well as high temperatures at which these phases exist. Where data are available, reliability is low due to the compromised accuracy of some of the methods employed in measurements (Kucharski et al., 1993; Tokumoto et al., 1972).

In an attempt to understand surface phenomena, a number of surface tension measurement methods have been developed. Drelich et al., (2002) recommended the gravity distorted drop methods (sessile and pendant drop) for direct measurement of molten metals at high temperature. The sessile drop method is based on a well-established equilibrium between gravity and capillary forces which can be related to the drop profile. The sessile drop method's advantage is due to its adaptability for measurements at high temperatures (Tiida and Guthrie, 1980; Drelich et al., 2002). It allows for more accurate determination of surface tensions over a wide range of temperature compared with the other methods used at high temperatures. This method allows simultaneous determination of contact angle, spreading coefficient, work of adhesion and density (Tiida and Guthrie, 1980; Drelich et al., 2002). Furthermore, both the mathematical treatment for calculating surface tensions from measured drop dimensions, as well as the experimental equipment needed for producing a sessile drop, are relatively simple (Tiida and Guthrie, 1980). Earlier, measurements by sessile drop were done manually which compromised accuracy. Because of this unreliability as well as inaccurate temperature measurements, researchers have opted to use other methods to perform measurements. However, the advantage of this

method is its flexibility to modification (Drelich et al., 2002; Eustathopoulos et al., 1999). Its suitability for surfactant solutions, viscous liquids and melted metals also makes it versatile. Principally, the method involves measurement of drop profile of the sessile drop that is placed on non-reactive horizontal substrate of very low surface roughness (in the order of 0.02 μm) (Eustathopoulos et al., 1999). It is recommended that substrates used in sessile drop measurements be poorly wetted by the drop, i.e., they should have a contact angle larger than 90 ^{o}.

1.3 Research questions and objectives

This work aims at answering the following questions: Is it possible to accurately measure surface tensions of mattes with the sessile drop method? How accurate are sessile drop method surface tension measurements compared with other experimental methods?

Therefore the main objective of this study is to develop a setup for sessile drop technique and use it to experimentally measure the surface tension of base metal molten matte phases in an inert atmosphere of purified argon on an inert substrate. This entails:

- Understanding the relationship between surface/interfacial tensions and the sulfide smelting operations, as detailed in literature.
- Critically reviewing the literature on the traditional sessile drop method to understand its suitability compared to other methods available for surface tension measurement.
- Developing a setup of a modified sessile drop method to accurately measure the surface tension of mattes in a simplified operation.
- Testing the new experimental setup for accuracy by performing surface tension measurements for Ni_3S_2, Cu_2S and FeS molten mattes and comparing the results obtained to those in literature.

1.4 Scope

In this project, the role of surface tension in matte-slag phenomena is discussed. Literature discussion assesses the relationship between surface tension and sulfide smelting. Surface tension measurements methods are reviewed with the focus on sessile drop method. A modified sessile drop method is developed for surface tension measurements.

The modification involves replacing parts of the optical system as well as the temperature measurement system of the traditional sessile drop method with a new and better one. The new optical system should be able to accurately and rapidly measure the surface tension with ease. It also involves modifying the temperature control and measurement system in order to have more accurate temperature readings. The tested modified sessile drop method is specifically applied to experimentally determine the surface tension of Ni_3S_2, Cu_2S and FeS molten mattes. The system investigated is: Gas (argon) – Molten matte (Ni_3S_2, Cu_2S, and FeS) – solid (alumina substrate). In this study, surface tension will be measured for Ni_3S_2, Cu_2S, and FeS molten phases as a function of temperature from melting to 1300 $^{\circ}$C.

1.5 Layout

This thesis will focus on the measurement of surface tensions of mattes in base metal (copper and nickel) smelting processes using a modified sessile drop method.

In Chapter 2, the theory of surface tension and its influence on the overall sulfide smelting operation will be reviewed. Various methods of surface tension measurement will also be discussed. This information will provide understanding on the necessary modification of the sessile drop method.

Chapter 3 presents the principle of the modified sessile drop method as applied in this study. Details on materials and procedure used are also presented.

In Chapter 4, the results obtained for the different systems in the study are discussed.

Finally, in Chapter 5, conclusions are drawn with recommendations for future research and action.

2 Literature review

2.1 Introduction

Copper is most commonly available in the earth's crust as sulfides and mostly containing iron, e.g. chalcopyrite ($CuFeS_2$), bornite ($CuSFe_4$) and chalcocite (Cu_2S). Primary nickel is also mainly produced from sulfidic ores. Globally, copper ores are now known to contain only about 0.5 – 2 % total copper. Because of this low copper content, the ores are often concentrated to higher grades of between 20 and 30 % copper. Smelting and refining proceed from this stage. About 90% of the world's primary copper originates from $Cu-Fe-S$ ores (Imris, 2003). Since $Cu-Fe-S$ minerals are insoluble in most aqueous solutions, most copper and nickel sulfides ores is extracted by smelting at high temperatures. (Davenport et al., 2002)

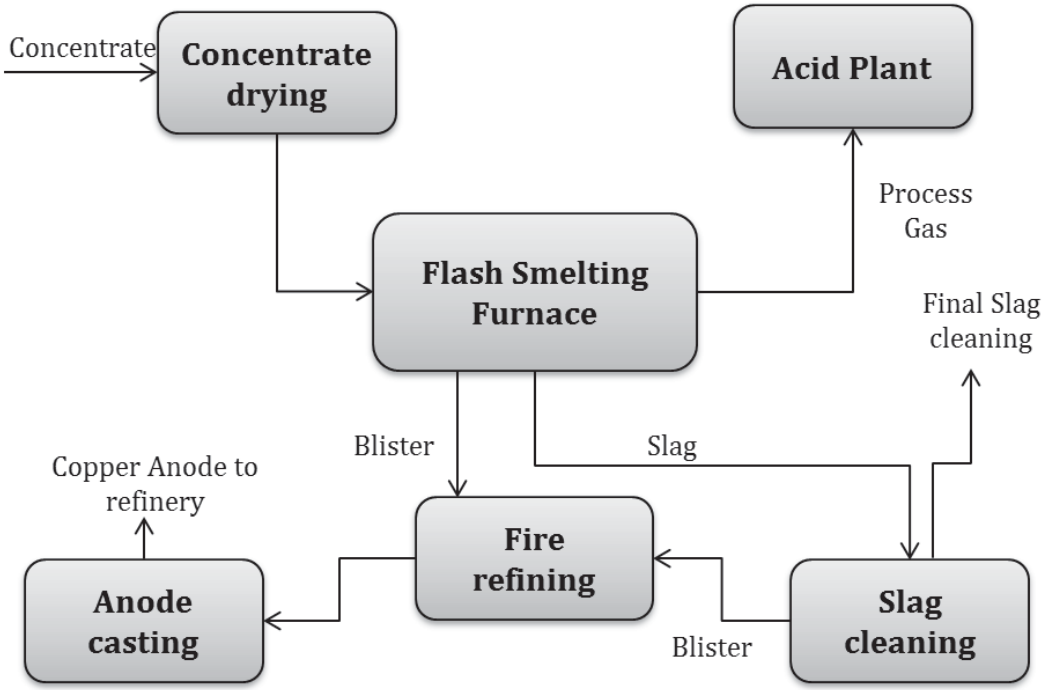

Figure 5: Outotec Direct to blister Cu flash smelting process flow sheet (adapted from Outotec, 2012).

2.2 Smelting

Smelting sulfide concentrate entails producing a molten high-Cu matte and converting the matte to an impure form of molten copper before electro refining to pure copper (~99.99%). Figure 5 shows a typical smelting flow

sheet. The slag obtained is a solution of molten oxides. Molten oxides include FeO from Fe oxidation, SiO_2 from flux and oxide impurities from concentrate. The settling of matte and slag takes place in the settler zone of the furnace and the overlay of matte and slag phases are shown in Figure 6, which depicts the Flash Smelting Furnace (FSF). During matte smelting of copper, the main copper matte formation reaction takes a general form:

$$CuFeS_2 + O_2 \rightarrow Cu - Fe - S_{(matte)} + FeO + SO_2 \qquad \text{Equation 3}$$

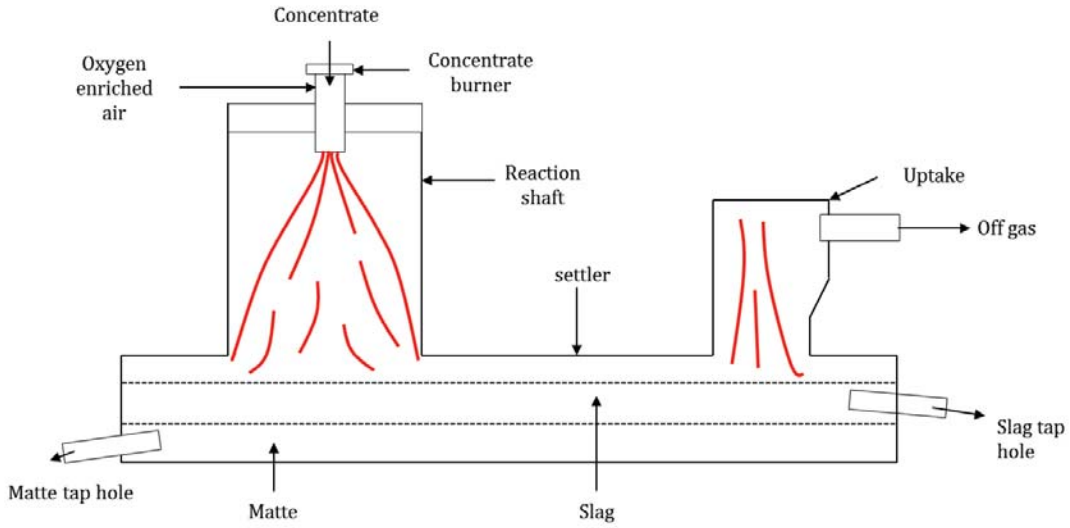

Figure 6: A cut- section diagram of the flash smelting furnace showing the settling of slag on top of matte (adapted from Vaarno et al., 2003).

At smelting temperature, the matte phase has higher density than slag and it settles at the bottom while the slag floats on top of matte (Mäkinen and Taskinen, 2006). One of the goals of smelting is to produce rich liquid matte phase and a liquid slag with less or no copper. This process also produces sulfur dioxide which is evolved as observed in Equation 3.This is an energy intensive process and takes place at higher temperatures (~1200 °C). This is a challenging task which requires knowledge of the physicochemical behaviour of both molten phases (matte and slag).

The sensitivity of many process parameters such as matte grade and how they impact on recovery means that successful smelting can only be achieved

when a balance is identified. For example, the use of excess oxygen leads to high matte grade caused by high oxidation of iron in the concentrates. The opposite of this is represented in Equation 4:

$$Cu_2S + \tfrac{3}{2}O_2 \rightarrow Cu_2O + SO_2 \qquad \text{Equation 4}$$

The result of reaction in equation 4 is unwanted to smelting because copper contained in this form is all lost to slag. One other important factor that is employed in copper sulfide smelting is controlling the activity of iron oxide (FeO) present in the slag. A high activity of iron oxide in slag results in Cu_2S breakdown as in Equation 5.

$$FeO_{(slag)} + Cu_2S_{(matte)} \rightarrow FeS_{(matte)} + Cu_2O_{(slag)} \qquad \text{Equation 5}$$

Again this results in loss of copper. Iron oxide can also react with oxygen as in Equation 6:

$$3FeO + \tfrac{1}{2}O_2 \rightarrow Fe_3O_{4(s)} \qquad \text{Equation 6}$$

Because of the need to lower the high activity of iron oxide, silica is usually introduced, see Equation 7:

$$FeO + SiO_2 \rightarrow FeO.SiO_{2(slag)} \qquad \text{Equation 7}$$

Whereas Equation 7 is an iron oxide activity control measure, this reaction has direct impacts on settling of matte droplets.

In a study of the surface tension of $Cu_xO - SiO_2$ slags in the air at 1300 °C by maximum bubble pressure method by (Nakamura et al., 1991), it was reported that the surface tension of the slag gradually decreased with a corresponding increase in SiO_2 content. In the study they observed that if the surface tension of pure oxide is higher than that of SiO_2, surface tension decreases with an increase of SiO_2 content. On the other hand, if the surface tension of pure oxide is lower than SiO_2 i.e., PbO, the surface tension of the binary silicates increases with an increase in SiO_2 content (Nakamura and

Toguri, 1991). The non-uniform effect of variation of SiO_2 in different molten silicate slags is depicted in Figure 7.

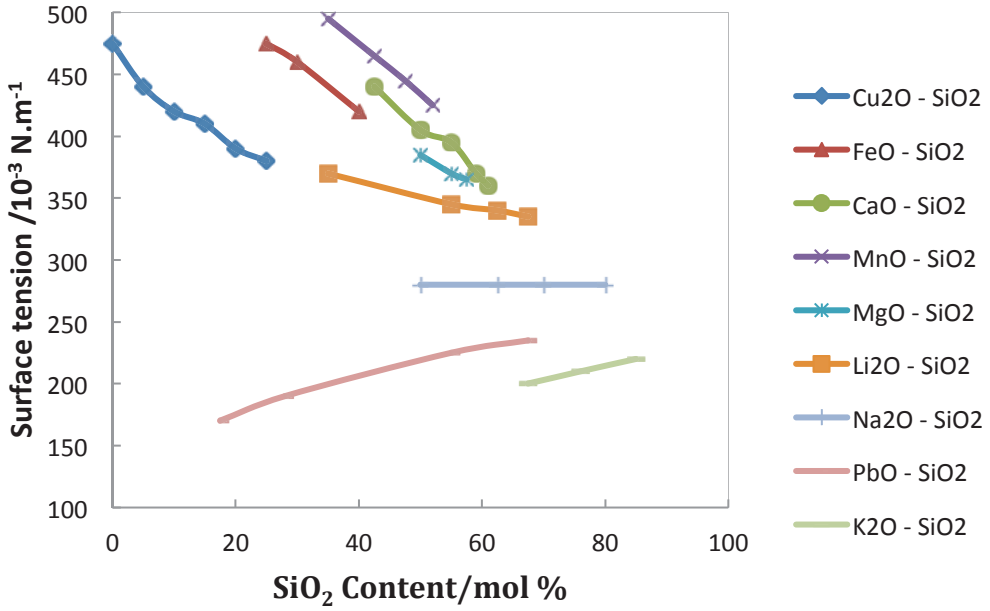

Figure 7: Dependence of surface energy on composition in various binary molten silicates at 1300 °C (adapted from Nakamura and Toguri, 1991).

2.3 Settling of copper matte and metal droplets in copper slag

Minto and Davenport, (1972) introduced a parameter termed the flotation coefficient which they combined with the Harkins spreading coefficient (Harkins,1952) to explain the mechanisms of formation of mechanically entrained matte droplets in slag. Equations 1 and 2 gives the spreading and flotation coefficients respectively.

$$\Phi = \gamma_{s/g} - \gamma_{m/g} - \gamma_{m/s} \qquad \text{Equation 1}$$

$$\Delta \approx \gamma_{s/g} - \gamma_{m/g} + \gamma_{m/s} \qquad \text{Equation 2}$$

Figure 8 illustrates different configurations of matte-slag at different coefficients (flotation and spreading) mentioned by (Minto and Davenport, 1972).

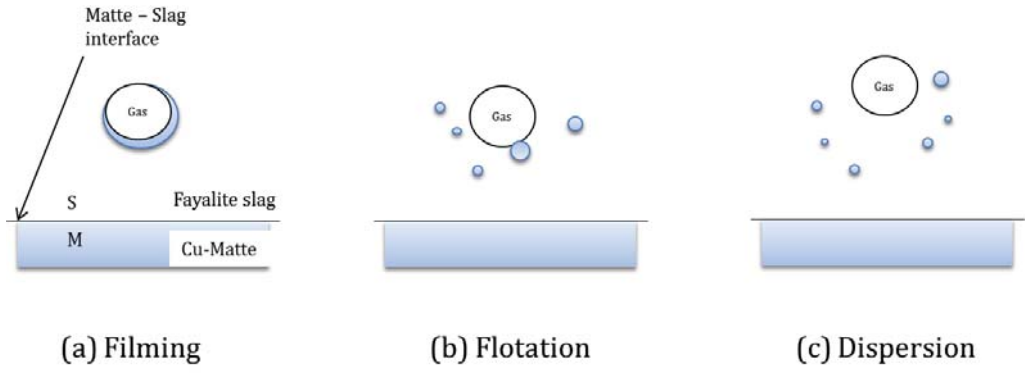

Figure 8: Schematic of Cu- matte loss into slag by gas bubble (adapted from Minto and Davenport, 1972).

In Figure 8 above, S and M are slag and matte respectively. In case (a), a metal or matte film will be stable on a gas bubble in the slag phase only when the spreading coefficient is above zero. Flotation (b) takes place when the spreading and flotation coefficients are negative. In the case of (c), dispersed metal or matte droplets will be expected when the spreading coefficient is negative and the flotation coefficient is higher than zero. From the coefficients given in Equation 1 and 2, it can be seen that data of surface tensions of molten copper mattes are necessary to calculate both coefficients in the matte - slag system, illustrated by the presence of $\gamma_{m/g}$ which is the matte surface tension.

2.4 Copper losses in the slag

Copper that is lost to slag during smelting of sulfides is generally in two forms, dissolved and mechanical. Metal lost by mechanical means is in form of droplets and can be explained well by Stoke's law. Properties such as surface tension, viscosity and density to a greater extent determine this loss. In practice, giving metal droplets more settling time has been observed to reduce metal losses to slag by mechanical entrainment. The effect of slag melting temperature as well as viscosity no longer applies when temperature is high. However, the amount of fuel used increases which results in increased costs. Therefore, a slag with low viscosity at lower smelting temperatures is ideal. Settling rate for matte droplets can also be explained using Stoke`s law:

$$v = \frac{2}{9} g \frac{\left(\rho_{drop} - \rho_{slag}\right)}{\mu_{slag}} r_{drop}^2 \qquad \text{Equation 8}$$

From Equation 8, v is the settling velocity of the matte droplet [cm.s^{-1}], g is the acceleration due to gravity, ρ_{drop} and ρ_{slag} are the densities of the matte and slag particles respectively [g.cm^{-3}], r_{drop} is the radius of the enclosed particles [cm] and μ_{slag} is the slag viscosity(Davenport et al., 2002).

From Equation 8, smaller droplets of matte settle slowly while larger ones will settle faster. During smelting, gas is infused in the matte slag system resulting in matte droplets being carried by gas bubbles to slag. At high flow rates of gas, there is disturbance of the matte slag phase which results in matte carrying gas bubble eruptions. These eruptions lead to an increased metal lost to slag. (Davenport et al., 2002).

Nakamura et al, 1991, studied the effect of oxygen partial pressure and made the conclusion that the spreading coefficients increase with increasing oxygen partial pressure. The increase in the value of the flotation coefficient with oxygen partial pressure is due to the decrease in the surface tension of copper with increasing oxygen pressure. The non-stable suspension of copper droplets with gas bubbles in copper slags is expected at low oxygen pressure since both coefficients are negative. However, as the flotation coefficient becomes positive at higher oxygen pressure suspension of copper due to gas bubbles should occur, see Figure 9.

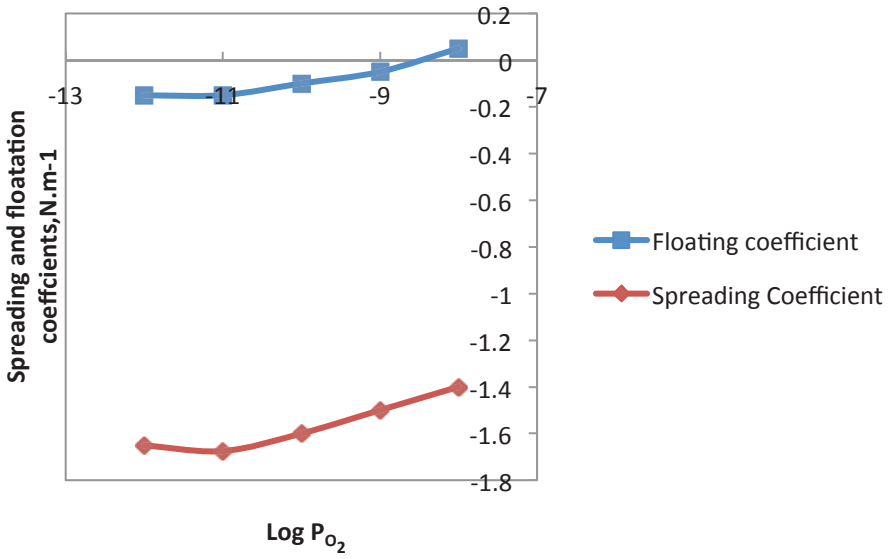

Figure 9: Effect of oxygen partial pressure on the spreading and flotation coefficient in the copper-fayalite slag system (adapted from Ip and Toguri, 1992)

The relationship between oxygen partial pressure and interfacial tension for copper is reported in Ip and Toguri, (1992). They deduced that between 10^{-12} and 10^{-8}, oxygen barely has affects interfacial. Ip and Toguri, (1992) observed a nonlinear correlation between the spreading and flotation coefficients and the oxygen partial pressure.

They also examined the flotation behaviour of various entrained phases by using spreading coefficients in conjunction with ternary interfacial diagram. They observed that matte grade variations as well as the slag Fe/SiO_2 ratio are insufficient parameters to eliminate metal loss to slag by gas bubbles.

2.5 Corrosion of refractories in copper smelting processes

The molten phase of matte and slag in base metal sulfide smelting is very corrosive. Because of this, smelting furnaces are lined with suitable refractory materials, obtained at a very high cost. It is therefore good smelter practice to run the furnace in a way that it preserves the lifespan of refractory. (Sergin and Lepinskikh, 1964) reported a refractory consumption of between 1 – 10 kg/ metric ton of copper produced. Refractory relining downtime directs translates in reduced productivity which undesirable.

Refractories are normally not damaged uniformly by melts such as matte and slag. It is more common that local corrosion of refractory occurs in the furnace at the slag line and the matte–slag interface. This is because of the interaction of phases. Studies have been carried out on the mechanism of local corrosion (Sergin and Lepinskikh, 1964). Mukai, (1985) has shown the importance of Marangoni convection in lead silicate systems.

When two liquids of different surface tension are placed together, a surface tension gradient forms and which makes the liquid with high surface tension flow towards the one with low surface tension, a phenomena referred to as Marangoni effect (Mukai, 1985).

In slag systems, presence of certain solute species has a significant effect on surface tension. Surface tension increases with increased solute concentration. In iron silicates slags for example, surface tension increase with alumina content (Nakamura and Toguri, 1991).

In smelting furnaces, intrusion of the molten slag into refractory lining leads to loss of thermal mechanical properties of the bricks, and it may lead to early failure (Fukuyama et al., 1997; Rigby, 1993; Barthel, 1993; Barthel, 1981; Ip and Toguri, 1993). The basic equation that explains the depth of intrusion of the melt into a capillary is:

$$h = \frac{2\gamma\cos\theta}{r\rho g} \qquad \text{Equation 9}$$

Where h is the depth of infiltration, γ is the surface tension of liquid, ρ is the density of liquid, θ is the contact angle between the liquid and the solid at the liquid surface, r is the radius of a capillary, and g the acceleration due to gravity. From Equation 9, the depth of infiltration is mostly driven by the surface tension and density of the molten phase (matte and slag) as well as the contact angle between the molten phase and the brick (Fukuyama et al., 1997).

Nakamura et al., (1991), also clarified local corrosion mechanisms in copper slag – matte system.

Figure 10 shows schematic diagrams of local corrosion mechanisms (adapted from Nakamura and Toguri, 1991) at the liquid surface. L_1 is the matte liquid phase.

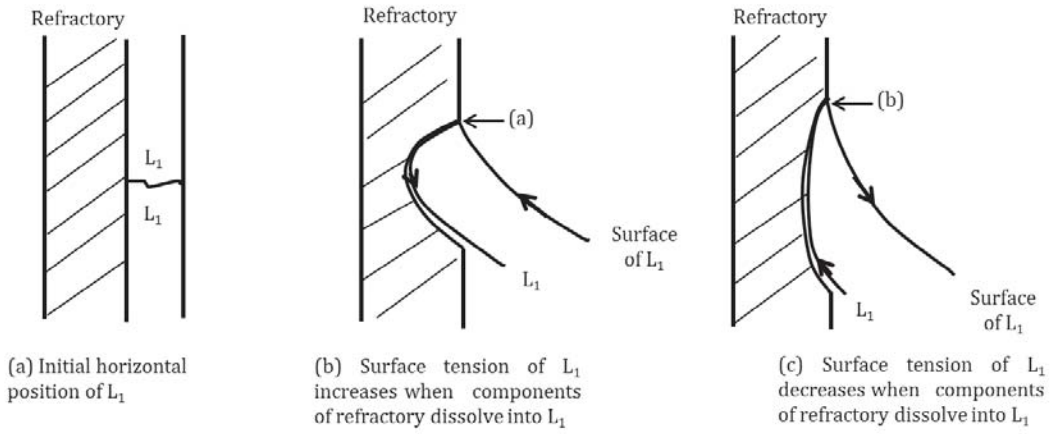

Figure 10: Schematic presentation of local corrosion of refractory by Marangoni flow at the liquid surface (adapted from Nakamura and Toguri, 1991).

The surface tension of L_1 increases due to dissolution of the refractory components into L_1. Because the surface tension of L_1 at point (a) in Figure 10(b) becomes larger than that of the bulk liquid, Marangoni flow occurs from the bulk surface to point (a). Figure 10 (c) shows the opposite case when Marangoni flow occurs from point (b) to the bulk surface.

Figure 11 shows schematic diagrams of local corrosion mechanisms (also adapted from Nakamura and Toguri, 1991) at the liquid–liquid interface by Marangoni convection. L_1 and L_2 represent molten slag and matte respectively.

If the interfacial tension between L_1 and L_2 decreases when the refractory components dissolve into L_1, Marangoni flow occurs from point (a) as shown in Figure 11 (b).

If the interfacial tension between L_1 and L_2 increases when the refractory components dissolve into L_1, fresh slag from the bulk flows to point (b) as

shown in Figure 11 (c). Such movement of slag at the interface gives rise to local corrosion of the refractory.

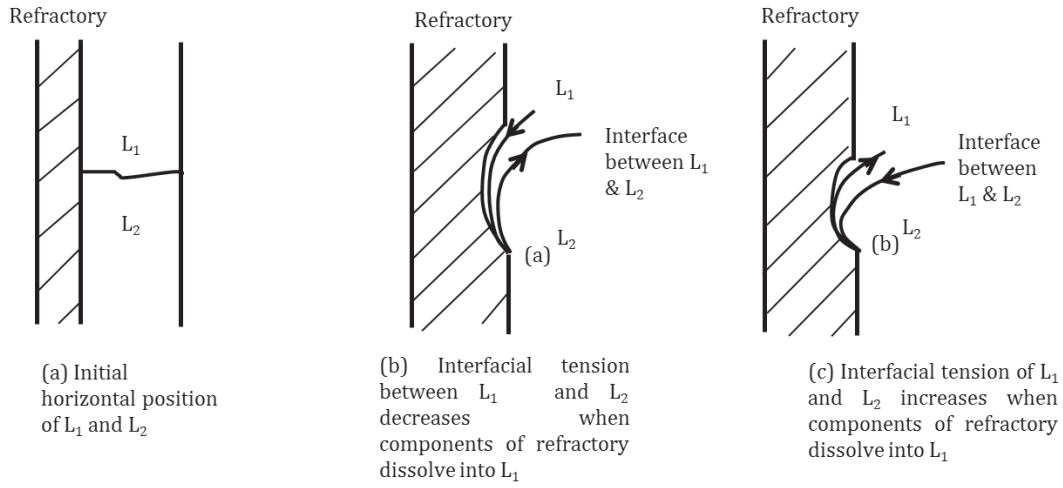

Figure 11: Schematic presentation of local corrosion of refractory by Marangoni flow at the liquid-liquid interface (adapted from Nakamura and Toguri, 1991)

2.6 The Marangoni effect

A summary of the basic knowledge and application of the Marangoni effect in high temperature systems is given in Mukai, (1985; 1992). The Marangoni effect describes how surface (or interfacial) tension differences or gradients, for example, in the x - direction, can affect the motion of liquid due to the generation of an interfacial shear stress between two liquids:

$$\tau_s = \frac{d\gamma}{dx} = \frac{\partial\gamma}{\partial T}\frac{dT}{dx} + \frac{\partial\gamma}{\partial c}\frac{dc}{dx} + \frac{\partial\gamma}{\partial\varphi}\frac{d\varphi}{dx} \qquad \text{Equation 10}$$

The surface/interfacial tension gradient is affected by the gradients of temperature T, concentration c of the surface active component in the liquid and electrical potential φ at the interface between two liquids. Liquid metals and slags generally have high surface or interfacial tension and strong surface active components such as oxygen and sulphur are generally present in liquid metal, both of which favour the occurrence of Marangoni convection. The Marangoni effect has been observed in molten slag systems in the following cases: (i) Marangoni convection due to temperature gradient (Nakamura and Toguri, 1991), (ii) Spreading and shrinking of slag droplets

on the metal due to changes in applied potential (Mukai et al., 1986). (iii) Marangoni flow of the slag film due to the concentration gradient (Mukai, 1998).

According to Seetharaman, (2005), The Marangoni effect by convection is more severe at liquid – gas and liquid – liquid interfaces. This aids mass transfer in areas of concentration in conditions where heterogeneous reactions are limited by mass transfer. The Marangoni effect's relationship to dilatational viscosity means it can be well related with many interfacial phenomena in metallurgy (Seetharaman, 2005; Matsushita et al., 2011).

2.7 The role of physicochemical properties in smelting processes

Smelting of sulfide concentrates is known to be driven by a number of physicochemical properties. The most influential physical properties are density, viscosity and surface tension of molten mattes (Davenport et al., 2002; Turkdogan, 1980; Tiida and Guthrie, 1988; Terek, 2000). At various conditions of temperature, composition and partial pressure, density, viscosity and surface tension of molten mattes, have been found to result into a specific outcome of the phase interactions. Quantification of the influence of matte and slag properties is essential for appropriate understanding and control of smelting processes.

Physical phenomena, such as emulsification of matte or metal, flotation of matte droplets into slag by the gas bubbles, slag foaming and the life of slag foam, have a great effect on the loss of valuable metal caused by physical entrapment in slag, and on the operation and control of the smelting process. Investigation of properties of matte and slag therefore becomes important not only for smelting efficiency and improvement of operations, but also for theoretical study of the smelting process (Jing et al., 1991).

2.7.1 Viscosity

The knowledge of viscosity of mattes and slags of various compositions and of its dependence on temperature for example, is essential for selecting the appropriate technology of metallurgical processes and methods for impurity

removal (Linchevsky, 1979). The viscosity of metallic melts determines the rate of diffusion processes in molten metal. The processes occurring during solidification of ingots and casting for example are linked inseparably with the viscosity of molten metal. Like density, viscosity is a structure-sensitive characteristic of the liquid state. Linchevsky, 1979 established that viscosity of liquids is dependent on free volume, i.e. on the structure of the liquid. Viscosity is inversely proportional to the free volume. At a larger free volume, the structure of the liquid is looser; i. e. the liquid is more free-running and has a lower viscosity (Linchevsky, 1979).

An understanding of the sensitivity of viscosity to temperature and composition in molten matte and slag system is important. In pyrometallurgical processes much attention has been paid to slag viscosity, with alloy and matte viscosities receiving much less attention.

Viscosity-temperature-composition relationships

The temperature dependence of the dynamic viscosity of the pure compounds Ni_3S_2, FeS, and Cu_2S can be seen in Figure 12.

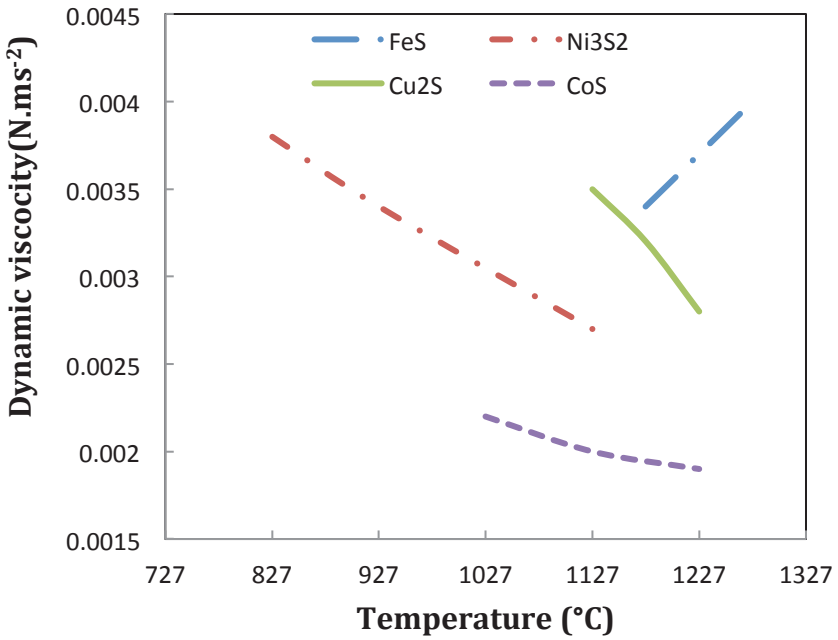

Figure 12: Dynamic viscosity of sulfide melts (adapted from Nikiforov et al., 1976)

Trends for Ni_3S_2, CoS and Cu_2S decrease almost linearly with an increase in temperature, while that of FeS increases unexpectedly. According to Nikiforov et al. (Nikiforov et al., 1976), the increase in the viscosity of FeS with temperature may be the result of the formation of structural complexes and the enlargement of structural units in matte. While it may seem strange to talk of structural units when referring to metallic liquids, liquid sulfide solutions are known to exhibit a high degree of short-range ordering (Kongoli et al., 1998). For this reason successful thermodynamic models of liquid sulfides (Kongoli et al., 1998; Waldner and Pelton; Kongoli and Pelton) have been developed using the modified quasi-chemical model of Pelton and Blander (Pelton and Blander, 1986), which was originally used to thermodynamically model molten oxide (slag) systems (Eriksson and Pelton, 1993; Wu et al., 1993), which are known to be ordered liquids (Sundström et al., 2008).

2.7.2 Density

By determining the relationship between density and composition of the melt for example, certain conclusions can be drawn on the structure of the liquid. Most structural transformations are accompanied by density variations. Analysis of the density of the liquids aids in understanding the structure of these complex solutions. (Turkdogan, 1980; Tiida and Guthrie, 1988; Linchevsky, 1979)

Knowledge of matte density is important for improving the accuracy of material balances in a smelter. Density data are useful for detecting solid spinel accumulation in smelting furnaces, which tends to accumulate at the slag-matte interface and is often tapped off with matte. Thus, with reliable matte density data this could be detected by measuring the density of the molten matte when tapped from the furnace. Density data also find use in mass and heat transfer calculations. The settling rate of matte droplets through slag can be calculated, and temperature or concentration gradients cause density variations that result in natural convection within a melt. As with viscosity data, knowledge of high-temperature density data is limited due to the experimental difficulties involved. (Sundström et al., 2008)

Experimental methods for density measurement

Among the various methods used for measuring the density of molten mattes, four have been investigated and their results compared. Some of the measurement techniques are the bottom-weighing Archimedean technique (Kaiura and Toguri, 1979), maximum bubble-pressure technique (Nagamori, 1969; Fujiswa et al., 1985; Liu et al., 1987), U-tube method (Byerley and Takebe, 1971; Azuma and Takebe, 1972), and the sessile drop technique et al., (1972).

The Archimedean method is based measuring the weight change of a calibrated bob immersed in the liquid phase whose density is being determined. The maximum bubble pressure method is based on the idea of a slow forming gas bubble at a tip of a capillary immersed in a melt, and measuring the maximum pressure in the bubble at the point where the bubble bursts (Kucharski et al., 1993, Sugden 1922). The U-Tube method is based on what is referred to as the Mass-Spring-Model, measuring the frequency of oscillation to be used to compute the density (Byerley and Takebe, 1971). Hyrn et al., (1996) evaluated many of the different methods. They found that the U-tube method is least accurate because the atmosphere above the matte sample cannot be purged. The gas that accumulates in this atmosphere may react with the melt and cause inaccuracies in the density measurements. The sessile drop technique is the simplest method to perform and allows measurement of density and surface tension at the same time, but may be slightly inaccurate due to the occurrence of small errors when analyzing the image of the matte droplet. Improved measurement methods offer scope to enhance the applicability of this method. Accurate data can be obtained when using the maximum bubble-pressure technique, which also allows simultaneous measurement of density and surface tension. This method may, however, be very difficult to perform, because the sulphur pressure over the matte sample must be controlled. The bottom-weighing Archimedean technique is also reliable, because the sample weight is continuously monitored. This means that compositional changes caused by sulphur can be detected (Hryn et al., 1996).

Byerley and Takebe, 1971, applied a least squares analysis to their experimental data on the O–S–Fe–Ni–Cu system, obtained by densitometer, to generate linear temperature density equations. Density equations revealed that the average drop in density for a 100°C temperature increase in the binary matte systems is about 0.2 g cm^{-3}. If density data are available at a single temperature, then it would be reasonable to assume a density decrease of 0.2 g cm^{-3} if the temperature is raised by 100°C, or that the density would increase with 0.2 g cm^{-3} if the temperature is reduced by 100°C.

With respect to sulfide systems, a ternary density diagram for the $Ni_3S_2 - Cu_2S - FeS$ system at 1200 °C was reconstructed from Kucharski et al., (1993), as shown in Figure 13. The addition of Cu_2S to the system has a weak effect on the density of the pseudo-ternary system, especially when the matte is rich in Ni_3S_2. It is apparent that the effect of FeS on the density of the pseudo-ternary becomes more significant at higher FeS concentrations. This is similar to the behaviour observed in the $Ni_3S_2 - FeS$ pseudo-binary system (Kucharski et al., 1993).

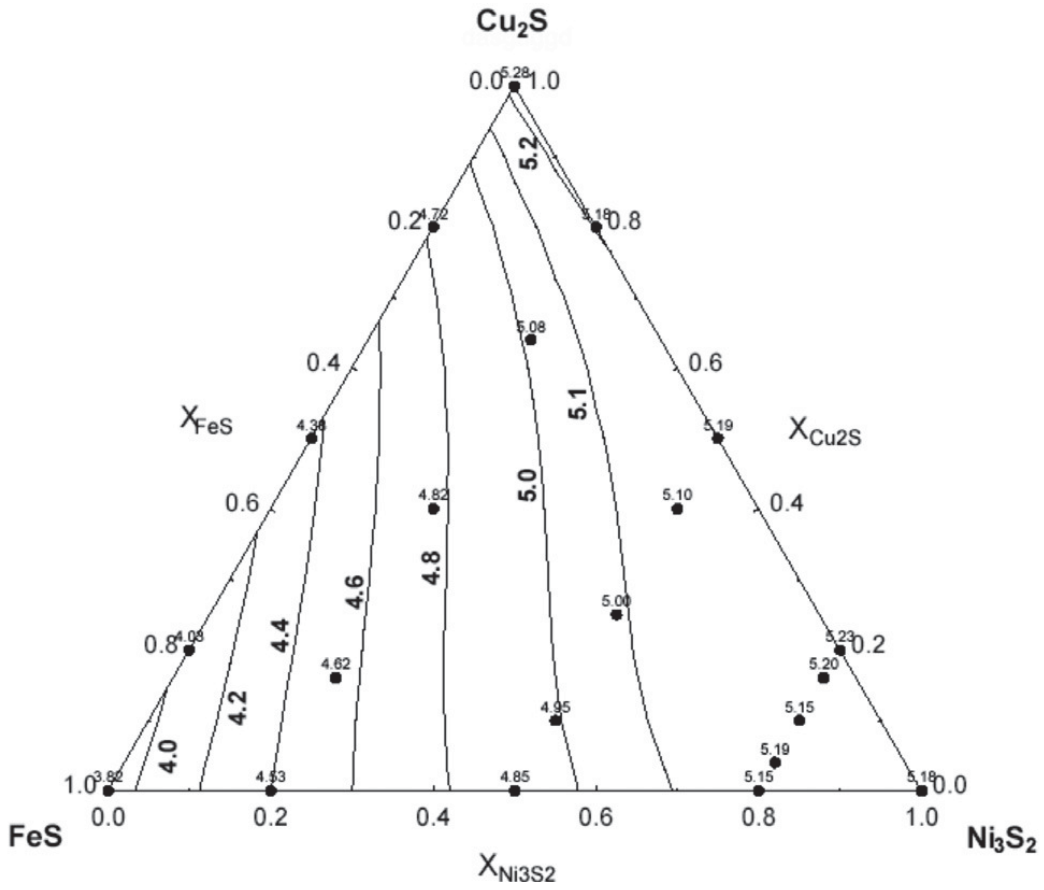

Figure 13: Ternary density diagram of the Ni_3S_2-Cu_2S-FeS system at 1200 °C. Experimental values are denoted by closed circles and the solid lines are iso-density lines (g.cm^{-3}) (adapted from Kucharski et al., 1993).

2.7.3 Surface tension

Thermodynamically, surface tension is that liquid surface property that by which it can resist external forces. Cohesive forces in this case present among liquid molecules are the major cause of surface tension. In the bulk of the liquid, see Figure 14, each molecule is pulled equally in every direction by a neighbouring molecule, which results in a net force of zero. However, molecules at the surface get stretched inwards due to lack of neighbouring molecules on one side. This creates some internal pressure and forces liquid surfaces to contract to the minimal area. This liquid behaviour is seen in the meniscus formed by liquids in containers.

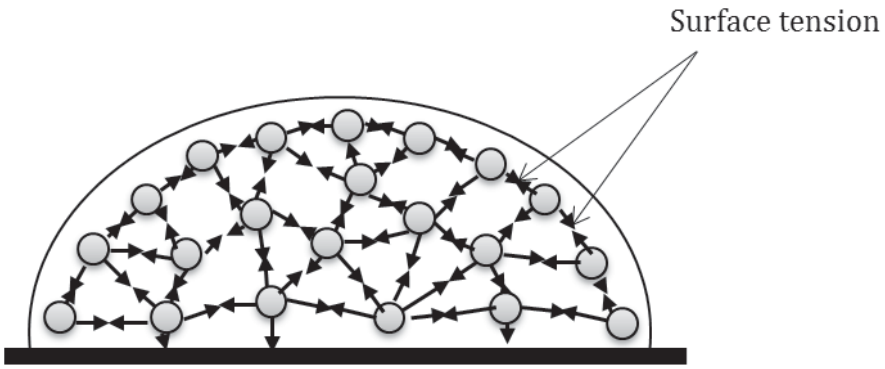

Figure 14: Cross section of a primitive three dimensional model of a material interfacing to vacuum (adapted from White, 1948)

In liquid droplets, surface tension can be seen as that force responsible for the resulting curved surface shape of the drop. This shape is as a result of an imbalance in cohesive forces caused by the unequal distribution of molecules, in the presence of gravity.

According to White, (1967), the difference in pressure across a curved liquid surface due to tension in the surface is related to the curvature and surface tension by the Young Laplace equation:

$$\Delta P = \gamma\left(\frac{1}{R_1}+\frac{1}{R_2}\right) \qquad \text{Equation 11}$$

Where

γ is surface tension of the liquid, R_1 and R_2 are the principal radii of curvature at a point on the liquid surface; ΔP is the pressure drop across the surface at the point.

Due to an imbalance in the intermolecular attractive forces, molecules in the interfacial area will possess more potential energy compared to the bulk phase (Thiessen and Man, 1999). From surface energy, the shape taken by the liquid surface can be easily understood.

Thermodynamically, an isolated system in equilibrium is said to be in its state of minimum free energy (Thiessen and Man, 1999). For multiphase

systems, surface free energy contributes to the combined free energy, Therefore, at equilibrium, surface free energy is minimized.

A new interface between two phases can be formed by expending a particular amount of energy which is equivalent to the acting force per unit length of the surface. For liquids, the surface energy is equal to the surface tension. In order to increase the interfacial area of one phase in another, work should be performed:

$$\partial A = \Delta p dV = \gamma dS \qquad \text{Equation 12}$$

Where Δp is the pressure gradient; V is the volume; γ is the surface tension and S is the area of a phase boundary. (Turkdogan, 1980)

Effect of bonding structure on surface tension

Mattes are covalently bonded, unlike oxides, chlorides or fluorides, which are predominantly ionic. The surface tension behaviour may therefore differ from that of common ionic melts (Mandira et al., 1987).

2.8 Surface tensions of binary and ternary phases

Molten metal during smelting has been found to exist in different phase systems such as binary, ternary, quaternary etc. For nickel and copper smelting, binary and ternary phase systems have been useful to better understand smelting (Turkdogan, 1980).

Surface tensions of some binary liquid alloys have been reported to vary nonlinearly with composition (Linchevsky, 1979). The departure from non-linearity is more pronounced in systems showing strong negative deviations from ideal thermodynamic behaviour, the Fe-Si is one such example.

Despite many attempts, there has been no general relation found to describe the composition dependence on surface tension. However, Eberhart in Turkdogan, 1980, has shown that for organic liquids, molten salts and some metallic solutions with modest departure from ideal behaviour, the following relation may be used for binary mixtures:

$$\gamma = (\phi x_1 \gamma_1 + x_2 \gamma_2)/(\phi x_1 + x_2)$$ Equation 13

where γ_1 and γ_2 are the surface tensions of pure liquid components 1 and 2, the coefficient ϕ, characteristic of the system, is determined by fitting the surface tension – composition curve to this equation.

Accurate measurement of surface tension is critical as its compositional sensitivity greatly affects slag-matte separation and the corrosive interaction of matte or slag with refractories. Reliable surface tension data would therefore assist in minimizing matte losses to slag and would be useful to describe the dependence of surface tension on composition.

From literature, only two methods were identified that have been used to measure the surface tension of mattes, namely the maximum bubble-pressure technique (based on the growing bubble) (Matsushita et al., 2005) and the sessile drop technique (based on a gravity-capillary equilibrium) (Mandira et al., 1987). The maximum bubble pressure method is based on the concept of a slow forming gas bubble at a tip of a capillary immersed in a melt, and determination of the maximum pressure in the bubble at the point of bursting (Kucharski et al., 1993; Sugden 1922). The sessile drop method uses the dimensions of a sessile drop of a liquid resting on a suitable substrate. The capillary – gravity equilibrium can well be related to these dimension of the drop by what is known as the Young Laplace Law. Both surface tension measurement methods can be used to measure density and surface tension simultaneously, as mentioned earlier.

Surface tensions of Cu_2S, FeS and Ni_3S_2 mixtures were measured using the maximum bubble pressure technique, and results are shown in Figure 15 and 16 (Kucharski et al., 1993). It was found that for the pure sulfides, the surface tensions are a linear function of temperature. For the pseudo-binaries, the surface tension behaved rather ideally with change in composition except for the $FeS - Cu_2S$ system. Pseudo is a term commonly used in equilibrium phase diagrams to describe portions of a true system. A pseudo-binary phase diagram is defined as an equilibrium diagram derived from a ternary or a

suitable higher-order phase system, such that phase boundaries resulting from the difference from two of the element contents are determined, and while contents of other elements remain the same. In the pseudo-ternary $Cu_2S - Ni_3S_2 - FeS$, Figure 15, surface tensions and molar volumes were not influenced strongly by the addition of Cu_2S to the system. FeS affected the surface tension at high concentration in the pseudo-ternary system (Kucharski et al., 1993).

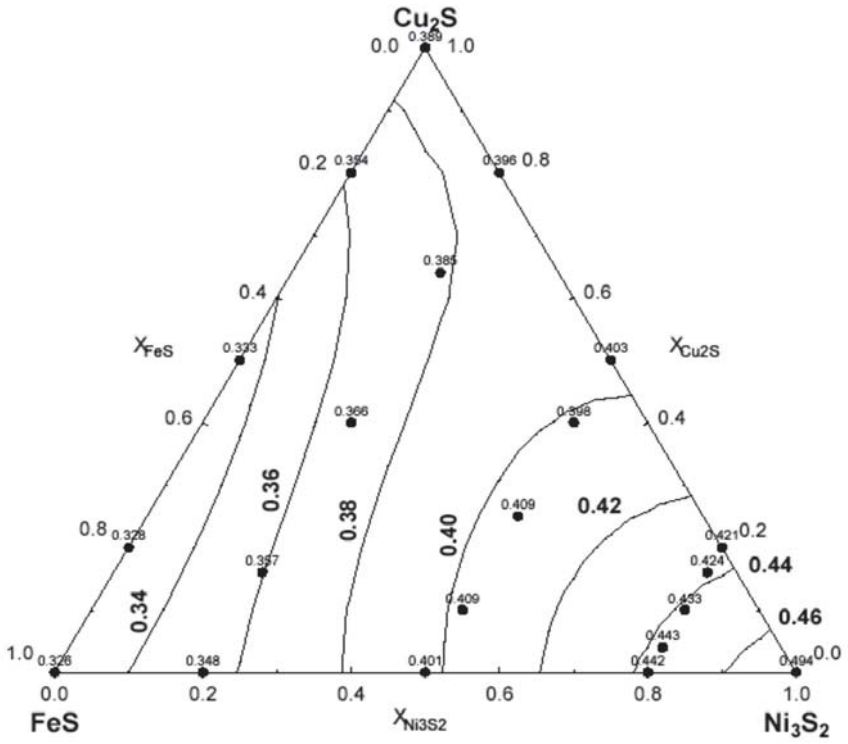

Figure 15: Ternary surface tension diagram of Ni_3S_2-Cu_2S-FeS system at 1200 °C according to the experimental data of Kucharski et al., (1993) Experimental points are denoted by the closed circles and the solid lines are iso-tension lines (N.m-1) (adapted from Kucharski et al., 1993).

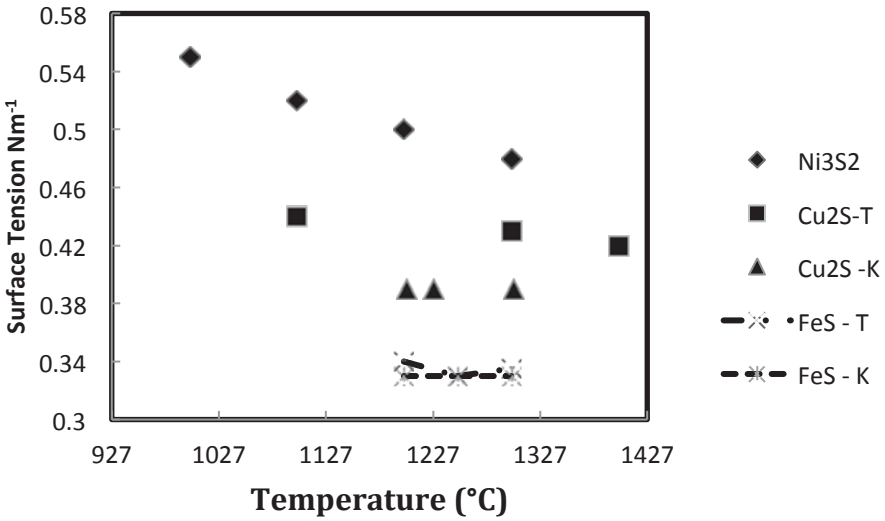

Figure 16: Effect of temperature on surface tension of pure matte compounds (adapted from Tokumoto et al., 1972; Kucharski et al., 1993.).

2.9 Surface tension measurement methods

White, (1962), Kozakevitch et al., (1959), Drelich et al., (2002), Eustathopoulos et al., (1999), reviewed the different methods of surface tension measurements at high temperatures. A summary of some of the classical surface tension measurement methods is depicted in Figure 17.

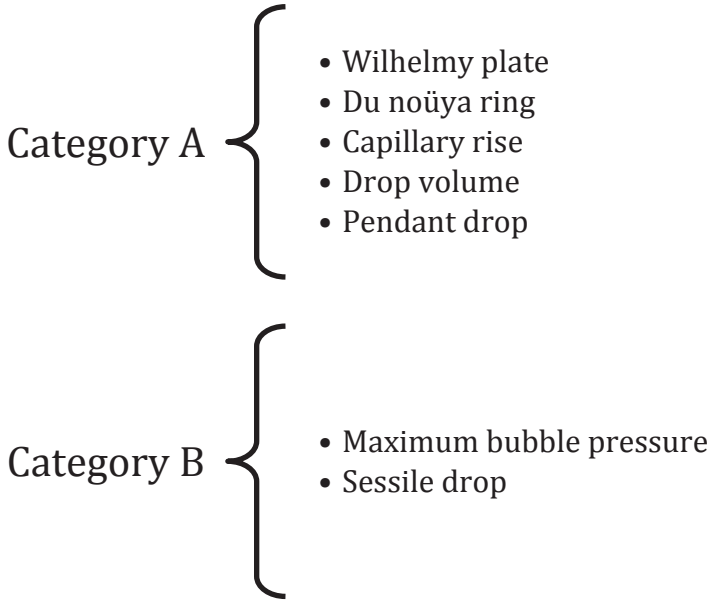

Figure 17: Classical surface tension measurement methods

Du Noüya ring and Wilhelmy plate surface tension measurement methods both work by applying the microbalance. According to Drelich et al., (2002), while the Du Noüya ring method is restricted to use as a detachment technique, the Wilhelmy method has been successfully applied for both static and detachment modes. Because of using the electro balance, Du Noüya ring and Wilhelmy plate have been applied by most researchers in cases where high precision in contact angles (for surface tension) is priority, for solids. However, the high sensitivity of the electro balance is exploited only when the surface of sample is uniform and this poses a challenge on non-uniform or partly uniform surfaces resulting in marginal errors.

Both the capillary rise and the drop volume methods of surface tension measurement employ the equilibrium established between forces of capillary and gravity. Because this equilibrium is well known, the methods have found much application and automation (Drelich et al., 2002). The capillary rise method for example, uses the height of the meniscus of a round glass tube of known radius. High accuracy values have been obtained (Keene, 1993). Despite these advantages, usage of transparent tube confines the method to

using glass or silica, which renders the method inapplicable for liquid metals at high temperatures. Another potential pitfall is accounting for distortion in meniscus profile by gravitational forces (Keene, 1993).

The other method of surface tension measurement is the pendant drop method. This method utilizes configurations of the shape that a liquid drop takes when it is suspended from an opening. This results from surface tension – gravity equilibrium of forces acting on this system (Keene, 1993). Images of a pendant drop are acquired and supercomputer profile fit methods are then applied to compute surface tension values. Practical problems of the pendant drop method include chemical compatibility of the materials in use, difficulties associated with measuring small dimensions as well as dealing with instability of detaching drop (Drelich et al., 2002, Keene 1993).

The maximum bubble pressure method is based on the concept of a slow forming gas bubble at a tip of a capillary immersed in a melt, and determination of the maximum pressure in the bubble at the point of bursting (Kucharski et al., 1993; Sugden 1922). The maximum bubble pressure method is suitable for determination of surface tension of molten mattes, and accurate results in this case have been obtained before (Kucharski et al., 1993). However, if the rate of the bubble formation is high, i.e. greater than one drop per minute, the mathematical treatment of this measurement method is no longer valid (Sugden 1922).

Another surface tension method that has been successfully used for molten phases is the sessile drop technique. In fact the sessile drop has been used to measure surface tension of melted mattes at high temperatures above 1200 °C in Tokumoto et al., (1972). In principle, the sessile drop method uses the dimensions of a sessile drop of a liquid resting on a suitable substrate. The capillary – gravity equilibrium can well be related to these dimension of the drop by what is known as the Young Laplace Law. Advantages of this method are compatibility with curve fitting techniques and easy automation, which results in elimination of possible human errors.

Despite the accuracy of most methods in Category A, surface tension measurement techniques only Category B methods have been successfully applied to measure surface tension of base metal molten sulfide mattes, at temperatures up to 1200 °C.

Table 1 gives a summary of some critical issues pertaining to surface tension measurements for different techniques.

The sessile drop method has an advantage due to its adaptability for measurements at high temperatures. Based on the droplet profile placed on a flat plane, this method allows measurement of surface tension and contact angle simultaneously. Another advantage of this method is its flexibility to modification because it is simple (Drelich et al., 2002; Eustapoulos et al., 1999). Its suitability for surfactant solutions, viscous liquids and melted metals makes it versatile.

Table 1: Accuracy and suitability of classical techniques used in surface tension measurements

Surface tension Measurement Techniques	Measurement Principle	Accuracy (mNm^{-1})	Type of Instrument (Manual or Automated)	Suitability for melted mattes at 1200°C	Commercial availability
Wilhelmy plate	Microbalance	~ 0.1	Both	Not suitable	Yes
Du Noüya ring	Microbalance	~ 0.1	Both	Not suitable	Yes
Maximum bubble pressure	Gas bubble formation	0.2	Automated	Yes	Yes
Capillary rise	Capillary & Gravity	≪ 0.1	Manual	Not suitable	Not
Drop volume	Capillary & Gravity	0.1 – 0.2	Automated	Not suitable	Yes
Pendant drop	Drop Shape	~ 0.1	Both	Not suitable	Yes
Sessile drop	Drop shape	0.1	Both	Yes	Not

2.10 The sessile drop method

There are five main requirements in successfully conducting a sessile drop experiment relevant to high temperature capillary phenomena: characterization of materials, a flat horizontal substrate, a test chamber to provide a controlled and generally inert gaseous environment, a facility that heats the sample to a predetermined temperature and a means of measuring the geometry and size of the sessile drop. In order to satisfy these requirements, care and precision in experimental procedures are needed. (Carla and Cecchini, 1991; Chirac et al., 1997)

2.10.1 Characterisation of materials

When conducting a sessile drop experiment, the researcher's main goal is to obtain reproducible results. Therefore, much as the surface tension values are needed, reproducibility of results is equally important. Characterization entails knowledge of material compositions especially the presence of surface active substances (Eustapoulos et al., 1999). The use of rough surface substrates for example, increases the contact angle values for most non-wetting system. The measure of the smoothness of material depends on the wetting characteristics of the system. According to Eustapoulos et al., (1999), Surface roughness of the order of 1μm has been used previously, but due to more demands of standards of smoothness, surface roughness of the order of 0.1μm is currently recommended and in use. The surface roughness of the order (0.1μm) gives an accuracy of ±2 – 3^{o} contact angle.

Material constituents of liquid phase and substrates as well as working experimental temperatures are important factors of the sessile drop method for surface tension measurement. This is because of a direct relationship that exists between material constituents and the attractive forces between molecules of the liquid (Eustapoulos et al., 1999). The surface tension of any particular liquid depends on the relative strengths of the intermolecular forces acting at the surface, which are governed by the chemical composition. For a specific liquid system, existence of certain consituents in small amounts

can significantly alter surface tension. Constituents that affect surface tension are called surface active, with respect to particular liquids. (Keene, 1993) describes surface activity of a substance as the surface tension per unit amount of constituents. From this relationship, the limiting surface activity is given as in Equation 14 below: of a solute x is given by the slope of the y ([x]) curve in the region where [x] approaches zero i.e.

$$J_L = \left(\frac{d\gamma}{d[x]} \right)_{[x]\to 0} \qquad \text{Equation 14}$$

In Equation 14, J_L is the limiting surface activity; [x] is the molarity of the constituents of surface active solutes. According to (Keene, 1993) this parameter is difficult to calculate, because even at low concentrations, it is still possible to incur minor errors due to issues associated with difficulty in precise material characterization.

2.10.2 Horizontal positioned substrate

When conducting a sessile drop experiment, for surface tension measurement, it is required that the substrate must be flat and horizontal. This helps position the drop symmetrically for equal contact angles at diametrically opposed location. If the drop is resting on a non-horizontal substrate, the molten phase will flow to the lower regions due to gravity. This will cause the drop to be distorted to two different values of contact angles of θ_a and θ_b respectively greater and smaller than required by the equilibrium condition that is defined by the Young Laplace equation; or in cases of very smooth surface to run down the slope, see Figure 18. (Eustapoulos et al., 1999)

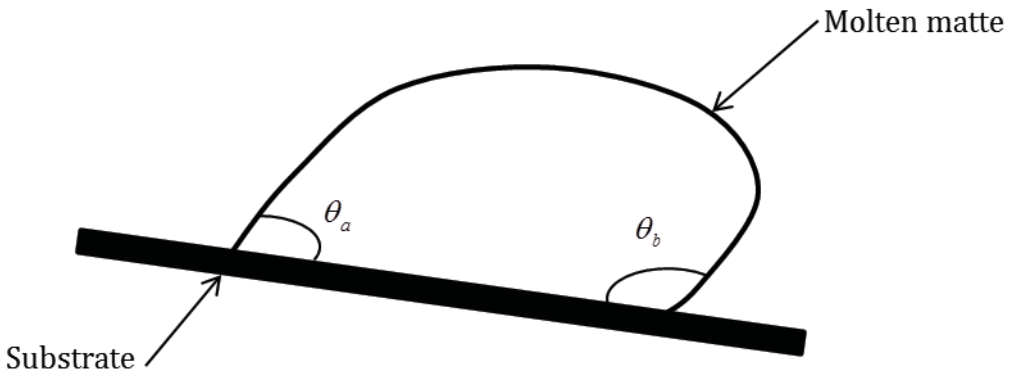

Figure 18: Effect of a tilted substrate (adapted from Eustathopoulos et al., 1999)

Distortion in the symmetry of the drops can also have effects in degrading the reliability of derived values of liquid surface energies; and can have some effects on the measured density values. The substrate surface must be flat or horizontal to avoid any movements when the solid cylinder melts to form a sessile drop (Eustapoulos et al., 1999).

2.10.3 Controlled gaseous environment

During sessile drop experiment, reactivity of species of the specimen must be controlled since it has an effect on the contact angles depending on substrate materials and presence of oxidizing species such as oxygen gas. Therefore, experiments are mostly done in inert atmospheres such as argon gas atmosphere (Eustapoulos et al., 1999). However, in most cases presence of oxidizing in traces i.e. 10^{-5} to 10^{-6} atm are permissible without altering contact angle. Most recently availability of inert gas purification techniques has reduced amounts of reactive gases. Sometimes controlled partial pressures are achieved by controlling the H_2/H_2O or carbon monoxide/carbon dioxide ratios. In this case, an electrochemical sensor is employed to verify the partial pressure for oxygen (Eustapoulos et al., 1999).

2.10.4 The effect of furnace atmosphere

The main known contaminant to the furnace atmosphere during the sessile drop experiment is oxygen. Oxygen in small amounts causes the creation of

an oxide film on droplets and this makes correct contact angle measurements difficult and therefore must be kept low (Eustapoulos et al., 1999). A specific oxygen partial pressure in this environment therefore will give a specific contact angle. At present, contact angle – oxygen partial pressure data is still scarce for most molten metal systems. For low oxygen partial pressure environments, sessile drop methods are performed in inert or vacuum atmosphere. But since most inert gases contain small amounts of oxidizing gases in the order of Po_2 10^{-5} – 10^{-6} atm in 1 atm, they must be purified. Usually when argon gas is employed for an inert atmosphere it is filtered through heated Zr shavings keeping the oxidizing gases to low levels (10^{-6} – 10^{-15} atm) where they cannot affect the experiment (Keene, 1993; Eustapoulos et al., 1999).

2.10.5 Sample heating facility

The mostly used methods of heating the sample and controlling its temperature are not specific to the sessile drop experimental method of surface tension measurement. Several heating methods and temperature control methods have been applied previously but most experiments have been conducted using electrical resistance heating elements which, ideally should be outside the test chamber to eliminate any possibility of contamination caused by evaporation or adsorption from their hot surface. This is more prominent when graphite heating elements are used since they are often porous. There must be additional care to achieve melting of liquid in quickest possible time especially when using alloys that have wide melting ranges. The heating rates should be fast (≥ 4 ^{o}C /min) through the temperature range to minimize premature wetting of a substrate due to migration of a liquid phase from a partially molten drop (Eustapoulos et al., 1999).

2.10.6 Sessile drop geometry measurement technique

Surface tension results obtained using the sessile drop technique are based on the geometry of the sessile drop i.e., drop profile and contact angle. In order for results to be accurate, some form of goniometer or optical system is needed to measure the contact angle as well as drop profile directly during

the experiment. Video and X- ray cameras have been used previously to achieve this. It therefore becomes essential to fit the heating chamber with observation ports, some of which should be in the same plane as the sample, and that the axis of the camera should be on the plane of the substrate surface. For this to be achieved, background illumination is usually employed mainly for visibility. However, at temperatures higher than 1000 ^{o}C (or less in some cases), there is no need for this illumination since the sessile drop will be luminous enough to be photographed optically (Eustapoulos et al., 1999).

2.11 Summary

Surface tension is an important factor in understanding mechanical entrapment of molten matte droplets into the slag as well as corrosion of refractories due to matte slag interaction. From literature, it is clear that several attempts have been made to study the phenomena of surface tension as it relates to metal making in the copper and nickel industry. However, success at high temperatures was only attained when using either the maximum bubble pressure or sessile drop method. On which method is more accurate between the two, it is still unclear. The sessile drop method is adaptable for measurements at high temperatures and could allow for more accurate determination of surface tensions over a wide range of temperature compared with the other methods used at high temperatures. Furthermore, both the mathematical treatment for calculating surface tensions from measured drop dimensions, as well as the experimental equipment needed for producing a sessile drop, is relatively simple. Its suitability for surfactant solutions, viscous liquids and molten metals also makes it versatile.

3 Materials and Method

3.1 Introduction

This chapter presents the principle, method, and materials employed in the surface tension measurements, by sessile drop method. The sessile drop apparatus presented here was built at Aalto University, School of Chemical Technology, in the Thermodynamics and Modeling Research Group. Sulfide powders were acquired from *Alfa Aesar* - A Johnson Matthey Company, in Germany.

3.2 Principle

For the sessile drop technique, surface tension of a liquid drop is obtained from the profile of the droplet combined with the forces of capillary and gravity, see Figure 19. The fundamental equation that describes this equilibrium for surface tension is known as the Young-Laplace Law.

The Young Laplace Law

The Young-Laplace Law for pressure discontinuity due to surface tension is given as:

$$\Delta p = \gamma\left(\frac{1}{R_1}+\frac{1}{R_2}\right) = \rho g z + c \qquad \text{Equation 15}$$

Where γ is the surface tension, R_1 and R_2, are the principal radii of curvature of the surface at any point *P*, ρ is the density of the liquid, c is a constant, Δp and is the pressure difference across the surface at that point. Figure 19 is a sketch of a meridional section of a liquid droplet.

If R is the radius of curvature of a meridional section, ϕ is the angle between OQ and PQ and if b is the radius of curvature at the vertex O, Equation 15 can be transformed into:

$$\frac{1}{(R/b)}+\frac{\sin\phi}{(x/b)} = 2+\frac{\rho g b^2}{\gamma}\frac{z}{b} \qquad \text{Equation 16}$$

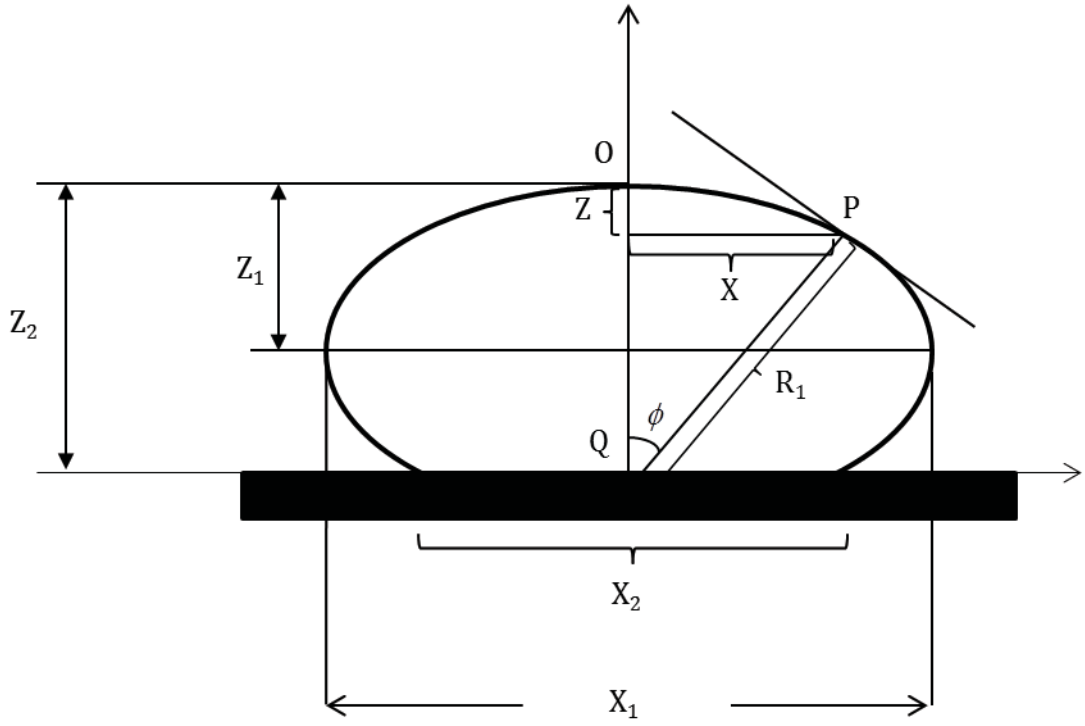

Figure 19: Definition of dimensions and coordinates describing the sessile drop (adapted from Tokumoto et al., 1972).

Hence, in order to simplify the Equation 16, assuming a 'shape factor' β equal to $\rho g b^2/\gamma$,

$$\frac{1}{(R/b)}+\frac{\sin\phi}{(x/b)}=2+\beta\frac{z}{b} \qquad \text{Equation 17}$$

Bashforth and Adamson, (1883) were the first researchers to put forth a numerical solution to the Laplace-Young equation. They tabulated the values of x/b and z/b for numerous values of β and ϕ, see Appendix I for a sample.

They found a number of numerical solutions to equation (17) by gradually adjusting β and ϕ for x/*b* and z/*b* for β for ϕ=90°. Using the dimensions x_{90} and z_{90} at ϕ = 90° values for β and *b,* are obtained. From Equation 18, surface tension of a particular liquid of known density is obtained.

$$\gamma=\frac{\rho g b^2}{\beta} \qquad \text{Equation 18}$$

The drop volume can also be calculated from their tables by measuring X_1 and Z_2. From this, the density could be calculated from drop weight and from drop volume.

Equation (17) gives some important parameters necessary for obtaining surface tension by sessile drop. Arithmetically results of surface tension can be obtained using estimation as obtained in the Bashforth and Adams's tables (Bashforth and Adamson, 1883).

The Bashforth-Adams equation's accuracy (Equation 17) has been proven; it is equally valid as the Young Laplace Formulation. A sample of typical solutions tables of the Young Laplace equation, called the Bashforth-Adams Integration tables (White, 1962) have been given in Appendix I.

3.3 Sample preparation

Pure sulfide powders of Ni_3S_2 (99.99 %), Cu_2S (99.99 %) and FeS (99.95 %), at -200, -200 and -100 Mesh respectively, employed in our measurements were purchased from Alfa Aesar (Germany). For compositions, see Table 2. The sulfide cylinders (droplets), whose diameter and length are 6mm and 5mm respectively, were prepared by using a hydraulic press, see Figure 20. Substrates of dense alumina (99.95), surface roughness of 0.1 μm, were used in the experiment. Measurements were performed in an inert atmosphere of purified argon at 20 ml per min. The purity of the argon gas was 99.999 %.

Table 2: Chemical analysis of Sulfides

Sulfides	Composition (Mass %)			
	Cu	Ni	Fe	S
Cu_2S	79.58	-	-	20.41
Ni_3S_2	-	69.53	-	30.46
Fes	-	-	63.87	36.08

When mixtures of sulfides were required for the binary and ternary systems, proportions of the pure sulfides were weighed and thoroughly mixed with a mixer and the sulfide cylinder (drops) were then prepared.

3.4 Experimental apparatus

Figure 20: hydraulic press for droplet preparation.

The experimental setup used in this study is depicted in Figure 21. It consists of an ENTECH, ETF 50 – 70/15 – S horizontal tube furnace with an alumina tube of 100 mm length, with inside diameter 40 mm (Figure 22). It is built with SiC heating elements placed parallel and around the tube. The furnace is manufactured to conduct experiments in inert environments and up 1500 °C. The argon gas used in the experiment was purified using two types of cartridges (Messer, Krefeld, Germany: Hydrosorb for moisture removal and Oxisorb for oxygen removal). This ensured oxygen partial pressures were kept low (less than 10^{-8} atm). This was compensated for by the fact that the composition of pure substances did not change over the considered period.

The temperature was measured by an S type (Pt - Pt 10 % Rh) thermocouple placed below the sample holder and near the sample (within 10mm). The thermocouple was calibrated using pure copper (known melting temperature). The ambient room temperature measurement was done with a Pt100 sensor (Platinum Resistance Thermometer) instead of a mercury

thermometer. The sensor was calibrated against ice water at 0.15 °C and the obtained resistance value was R_0 = 100.013 Ω. This value was entered into NI LabVIEW temperature logging program. The manufacturer reports that the tolerance of the sensor is in accordance with the DIN IEC 751 standard B1/10 and obtains an accuracy of ±0.03 °C.

The sample holder with sulfide specimen on substrate was placed in the hot zone furnace tube using a pulling rod. Temperature profiles were obtained to ensure the droplet formed was within ± 1°C (5mm) identified zone. It was observed that the length of the uniform temperature zone is approximately 70 mm. The sample holder allows movements for horizontal positioning of substrate. For visibility of the droplet and illumination, the furnace tube was fitted with borosilicate glass at both ends. A system's insulation consisted of a rectangular shield (Thick gauge mild steel with a ceramic fiber blanket inside) which insulates the furnace and minimize loss of heat.

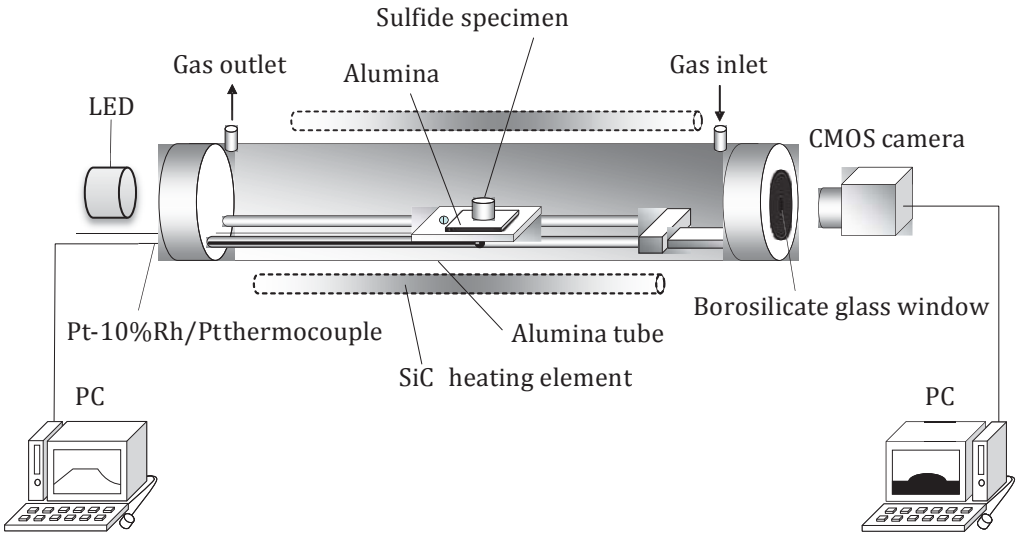

Figure 21: Schematic setup of experimental apparatus

The special optical system used was acquired from SKS Vision Systems Oy of Finland. VISI50 SMART Integrated machine vision sensor was used to record the image of the drop's contour (Vision systems manual). This is an

integrated machine vision sensor for measurement and quality control. It has been mainly used commercially for Edge position measurement, Center position measurement, Width measurement, Area measurement, and Object counting. The optical system used in this study, employs a high definition CMOS (complementary metal oxide semi-conductor) (Vision systems manual). The 5 megapixel camera has high performance in image processing tasks. For example, the user has an option to either use it as an area or line scan camera depending on the application. The high resolution translates into measurements of high accuracy. The equipment can also be supplemented with external illumination for certain applications. Object illumination as an option is done only in cases where natural light is insufficient (Vision systems manual). Object illumination may be done with integrated Light emitting diode (LED) or with other light sources. In our experiments, the device was connected to an automation system and LED light was used for illumination. However at high temperatures (above 1250 °C) there was no need for this light since the molten sulfide droplet is visible enough.

Figure 22: ENTECH, ETF 50 – 70/15 – S horizontal tube furnace (side view), Showing CMOS –HD camera (1), LED (2), and gas (3) and cooling lines (4) on both ends

VISI50 SMART integrated machine vision sensor has a compatible image acquisition system. It allows for data collection varieties such as a movie or images and these images can be saved in a format in real time with minimal alterations. At the same time the temperature is measured using an RS-232 serial interface Keithley 2000 digital multimeter. The image data obtained is stored to files and used to calculate surface tension. For surface tension calculations, FTA32 Software program (supplied by Crelab Instruments, Sweden) was employed using the dimensions of the droplet at a set magnification.

3.5 Density estimation

One important parameter, which must be known in calculations of surface tension, is the density of the matte droplet. Density values used in this study were adapted from the work by Kucharski et al., 1993, see Equations 19, 20 and 21 ($1000 < T < 1300$). Temperature is in °C.

$$\rho_{Ni_3S_2} = 6.144 - 6.6\times10^{-4}T \qquad [\text{g.cm}^{-3}] \qquad \text{equation 19}$$

$$\rho_{Cu_2S} = 6.075 - 5.4\times10^{-4}T \qquad [\text{g cm}^{-3}] \qquad \text{equation 20}$$

$$\rho_{FeS} = 5.435 - 1.1\times10^{-4}T \qquad [\text{g cm}^{-3}] \qquad \text{equation 21}$$

3.6 Procedure

The first step involved calibration of the optical system. A solid stainless steel cylinder with known dimensions was placed on the substrate and this sample system was placed in the uniform temperature zone with the pulling rod. Magnification of the optical system could be set whilst observing the image of the drop on a computer screen, in the presence of light provided by the LED. This adjustment also entails positioning the droplet in the center whilst getting a clear image. The magnification was set to obtain images of the order 640 x 480 pixels. The drop in the images used for the calculations occupied 75 %. The actual diameter of the drop was measured using a

vernier caliper while a measured diameter is obtained on the image in software. By using the two dimensions (actual and measured), the magnification was obtained. Once all the parameters were obtained, surface tension was calculated using Young Laplace equation method (Equation 15, 16, 17, 18) (Bashforth and Adamson, 1883). When the calibration had been done, the droplet, resting on the substrate was carefully placed horizontally in the uniform temperature zone with the help of a pulling rod.

At this point, the furnace tube was closed. The experiments were conducted under controlled partial pressure of oxygen. Oxygen partial pressures were estimated using HSC software to ascertain the environment and results are given in the results section. A high flow of purified (80 ml per min) argon gas was flushed through the furnace to remove oxygen and any other possible reactive gas, for 30 minutes. This flow rate was reduced to 20 ml per minute during the experiment. It was observed in preliminary experiments that a flow rate of 5 ml was not sufficient. The furnace was heated to the set point at a rate of 4 °C per minute. The temperature was held for another 30 minutes at set point to ensure the system had enough time to reach equilibrium. This time was arrived at after preliminary results indicated the system had equilibrated after 20 minutes. Figure 23 (a) and (b) depicts the drop image profiles of matte at the beginning and end of the experiment. For measurements of surface tension at temperatures higher than 1250 °C, there was no need for extra illumination as the droplet was visible without additional light.

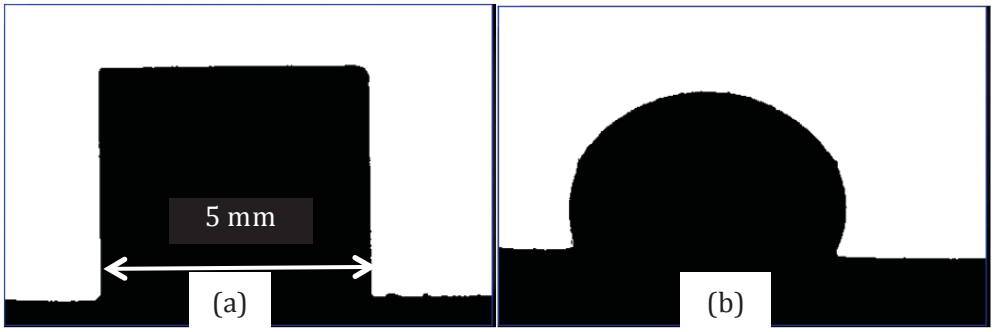

Figure 23: Binary images of initial and equilibrated matte droplet of Ni_3S_2 in (a) and (b) respectively (a) is at room temperature while (b) is at 1200 °C.

3.7 Temperature profile estimation

In order to identify the hot zone in the furnace where there is a desired temperature zone to conduct the experiments, the temperature profiles of the furnace were done across the whole length of the furnace tube at three different temperatures; 800 °C, 1100 °C, 1400 °C and are depicted in Figure 24. As can be seen, at about 60 cm from the end of the furnace, there is a well-developed hot zone. Therefore, all the sulfide specimens which pressed to a cylinder shape having 5mm in diameter and 5 mm in height were positioned at 60 cm during experiments.

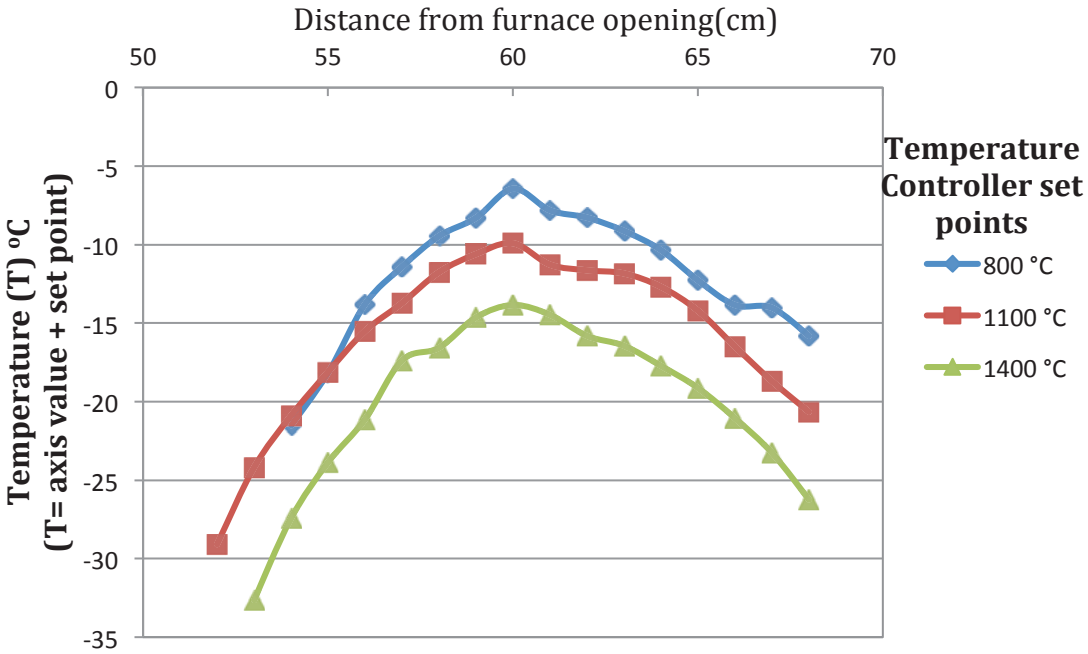

Figure 24: Furnace thermoprofile at different temperatures

4 Results and Discussion

4.1 Introduction

After the apparatus for the modified sessile drop method for surface tension measurements was developed and the tests were conducted, calculation of the values was done in software using a numerical solution of the Young Laplace equation at the surface of the drop. The results are given in this chapter. The surface tension of mattes as a function of temperature and composition is discussed and the results are validated with those available in literature. The results on the effect of oxygen partial pressure on the experiments are also discussed.

4.2 Surface tension of Ni_3S_2

Surface tension dependence of the Ni_3S_2 matte on temperature was obtained for temperatures ranging from 1000 ^{o}C to 1300 °C, when the system reached equilibrium. The point where no more changes to the drop profile take place defines this equilibrium (see Figure 33, Appendix IV). The surface tension of the molten Ni_3S_2 matte was measured in this temperature range (1000 °C – 1300 $^{\circ}$C), because it is critical to the smelting and converting of nickel/copper concentrates and mattes respectively. The results of the surface tension measurements on molten mattes for Ni_3S_2 are shown in Figure 25.

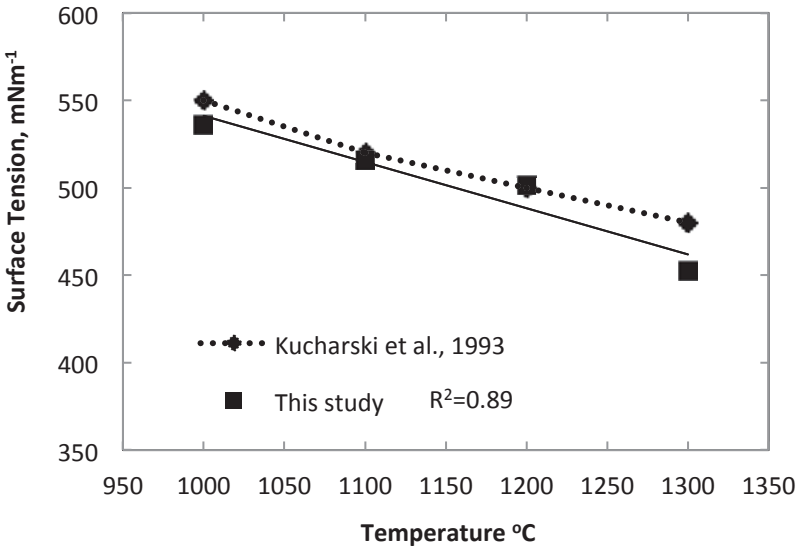

Figure 25: Effect of temperature on surface tension of Ni_3S_2

Each point on the graph in Figure 25 represents the average value from 15 independent experiments. The average values are shown in Table 3.

Table 3: Results of surface tension measurements for Ni_3S_2

Temperature (˚C)	Experimental (mNm^{-1})	σ (mNm^{-1})	Literature(η) (mNm^{-1})	% Difference
1000 ±2	536.23	-	550	2.50
1100 ± 1	513.93	6.10	520	1.17
1200 ±1	500.00	5.94	500	0.00
1300 ±1	452.82	-	480	5.66

σ is the standard deviation of the experimental results at each temperature. % Difference, is the difference between literature values (mNm^{-1}) and experimental values of present study, and is given by the following equation:

$$\%Difference = \frac{\overline{X} - \eta}{\eta} \times 100 \qquad \text{Equation 22}$$

where $\overline{X}$ is the mean of the current experimental values and η is the literature values. As can been seen from Table 3, there is a good correlation with the literature values, the highest percentage difference being around 5%.

From Figure 25 and Table 3, it is clear that the surface tension of Ni_3S_2 decreased linearly with an increase in temperature within the temperature range considered.

4.3 Surface tension of Cu_2S

Surface tension dependence on temperature was plotted after the system had reached equilibrium. The surface tension of the molten matte was measured in the temperature range 1200 – 1300 °C which is critical in most copper smelting operations. The results of the surface tension measurements on molten matte of, Cu_2S system are compared with those of Tokumoto et al., (1972) and Kucharski et al., (1993) shown in Figure 26. It is worth noting however that Kucharski et al., (1993) used the maximum bubble pressure method.

For Cu_2S (Figure 26 and Table 4), there is negligible temperature dependency.

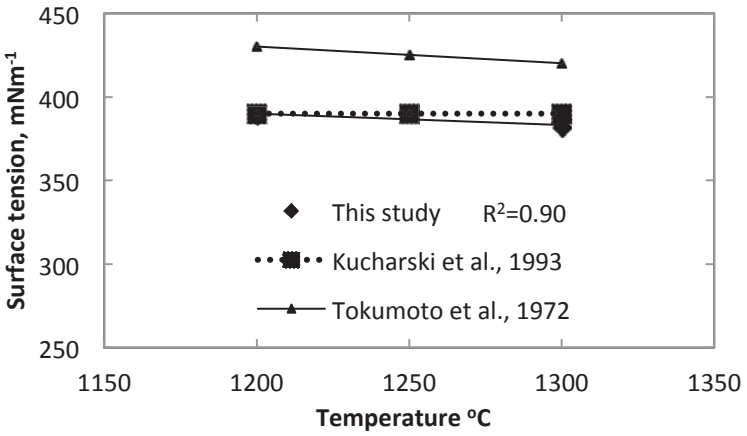

Figure 26: Effect of temperature on surface tension of Cu_2S

Table 4: Results of surface tension measurements for Cu_2S

Temperature (°C)	Experimental (mNm^{-1})	σ (mNm^{-1})	Literature(η) (Average) (mNm^{-1})	% Difference
1200 ±1	385.77	13.68	410.0	5.91
1250 ±1	385.00	19.53	407.5	5.52
1300 ±1	381.94	22.86	405.0	5.69

4.4 Surface tension of FeS

The results of the surface tension measurements on molten *FeS* are shown in Figure 27 and Table 5. The surface tensions were measured in the temperature range 1200 – 1300 ˚C, and the results are compared with literature.

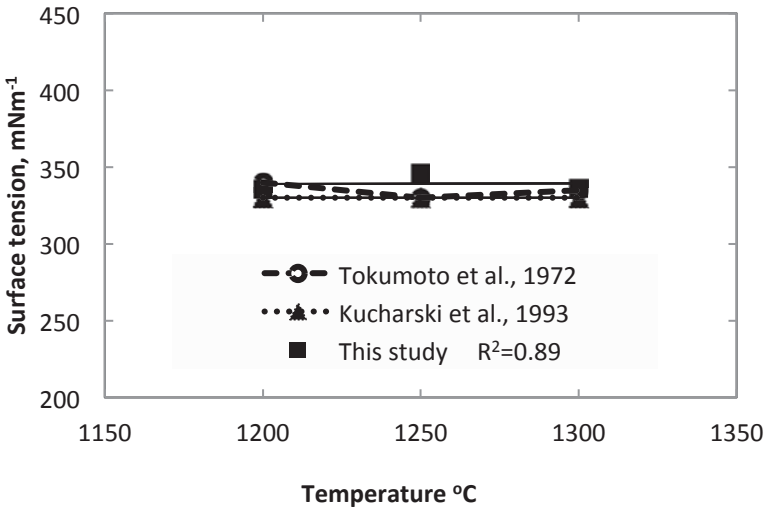

Figure 27: Effect of temperature on surface tension of FeS

The results presented in the Figure 27 and Table 5 for *FeS* are compared with those of Kucharski et al., (1993) and Tokumoto et al., (1972).

Table 5: Results of surface tension measurements for FeS

Temperature (°C)	Experimental (mNm^{-1})	σ (mNm^{-1})	Literature(η) (Average) (mNm^{-1})	% Difference
1200 ±1	332.24	13.02	335.0	0.82
1250 ±1	343.23	9.97	330.0	4.01
1300 ±1	334.39	8.57	332.5	0.57

4.5 Summary

For Ni_3S_2, the results compared well with those obtained by Kucharski et al., (1993) with a % difference of only up to 5.66. This can be attributed to the

difference in the methods used. Kucharski et al., (1993) used the maximum bubble pressure method to measure the densities and surface tensions of molten mattes. The results by sessile drop technique in this study are reliable and accurate based on the number of experiments conducted. In Kucharski et al., (1993), only up to four experiments were conducted for repeatability. This method used in this study provides for rapid data collection, which provided more (15) points of measurements, improving the accuracy. Drelich et al. (Drelich, 2002) compared the accuracy of various surface tension measurement techniques, in his findings; the accuracy of the maximum bubble pressure method is in the order of 0.2 mNm^{-1} while that of the sessile drop method, is in the order of 0.1 mNm^{-1}. There is good agreement between the results of this study and that of Kucharski et al, (1993), for all sulfides (% Difference ≤ 5.91 %). There is a deviation of up to 5.91 % in the Cu_2S measured results to those by Tokumoto et al., (1972). This could be due to the difference in the purity of the substances as well as the density values used in the calculations. A percentage difference of 5.91 was the highest recorded between the experimental and literature results. The high standard deviation in Cu_2S results, were caused by poorly shaped profile of the drop at temperatures above 1250 °C. However, this deviation presents a percentage error of 5.91 which is contrary to the 10 % observed by Tokumoto et al., (1972).

4.6 Surface tension of binary and ternary systems

The surface tension of Ni_3S_2-FeS, Cu_2S-FeS, Cu_2S-Ni_3S_2, pseudo-binary systems and FeS-Cu_2S-Ni_3S_2, pseudo-ternary system was also determined. Surface tension measurements of various compositions were done at 1200 °C at which point the system had reached equilibrium. At this temperature, all matte phases were in liquid form. Figures 28, 29, 30, illustrate the binary system results obtained from experiments. Each point on the experimental results of this study represents 10 independent experiments.

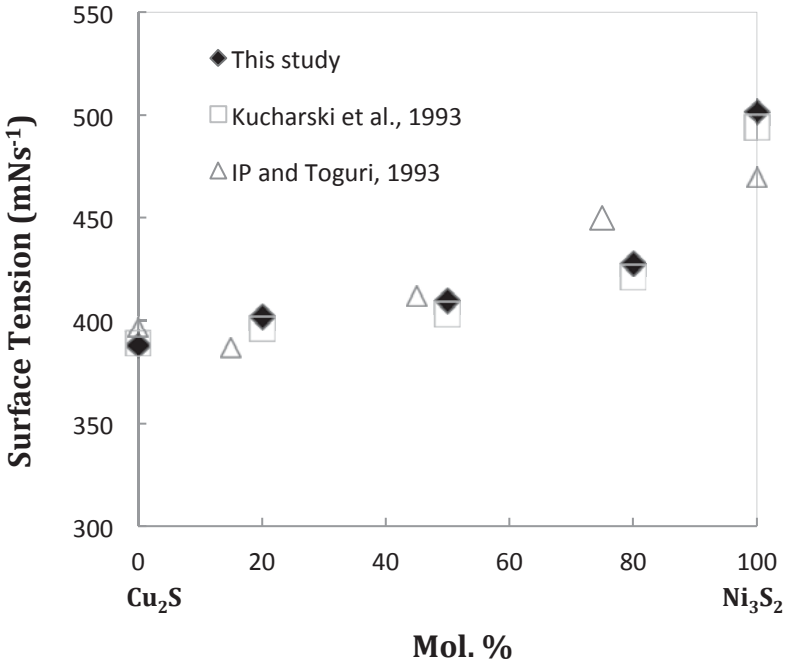

Figure 28: Isotherm of surface tension of Cu_2S-Ni_3S_2 system at 1200 °C

From Figure 28, 29, and 30, the sensitivity of surface tension to amounts of Ni_3S_2 *in* pseudo-binary systems is observed. The surface tensions of the three pseudo-binary systems increase with a corresponding increase in the amount of Ni_3S_2. Figure 28 and 30 show a nonlinear relationship while Figure 29 has a linear relationship with an R^2 value of 0.98 i.e., the linear model explains 98% of the variability in the data. The effect of Cu_2S in the Cu_2S-*FeS* pseudo-binary system is not negligible as seen in Figure 30. The results of binary systems compare well with those of Kucharski et al., (1993).

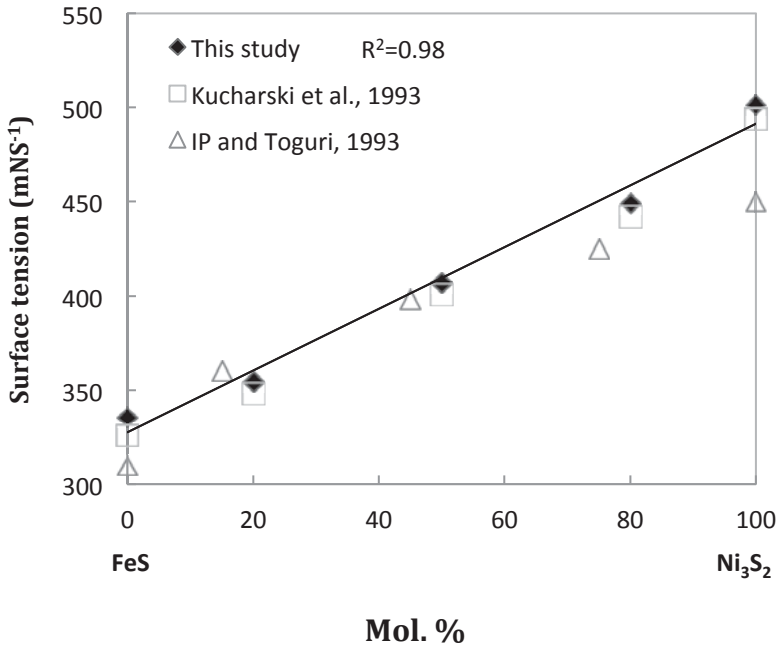

Figure 29: Isotherm of surface tension of FeS-Ni_3S_2 system at 1200°C

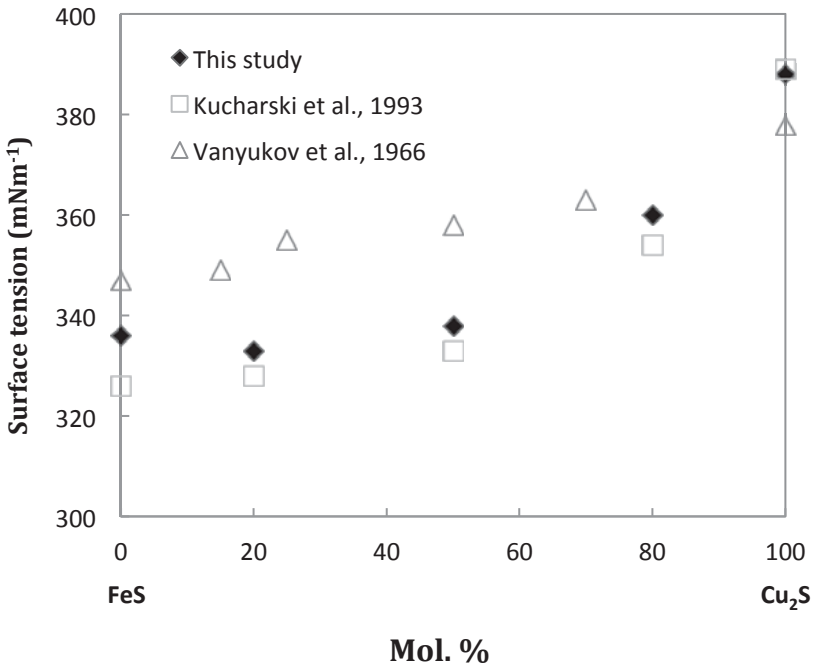

Figure 30: Isotherm of surface tension of FeS-Cu_2S system at 1200 °C

Figure 31 illustrates the surface tension results obtained from *the FeS-Cu_2S-Ni_3S_2* pseudo-ternary system. The numbers on each of the closed circles represents the surface tension at a point in mNm^{-1}. It can be observed that the surface tension of mattes varies with respect to composition, particularly the amount of *Ni_3S_2*. As can be seen, the surface tension increases with an increase in *Ni_3S_2* content, especially towards the *Ni_3S_2* rich corner of the pseudo-ternary diagram.

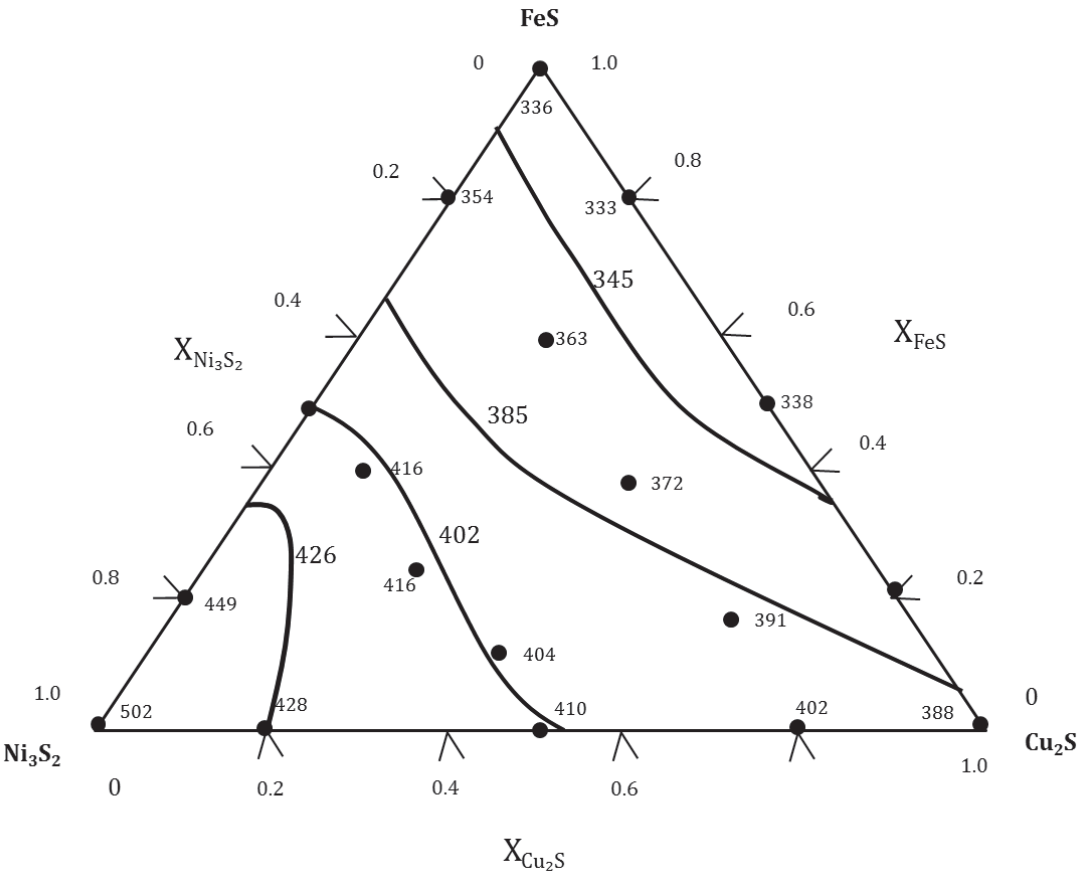

Figure 31: Pseudo-ternary surface tension diagram for the FeS-Cu_2S-Ni_3S_2 system (Mol. %) at 1200 °C, Surface tension and iso tension values in mNs^{-1}

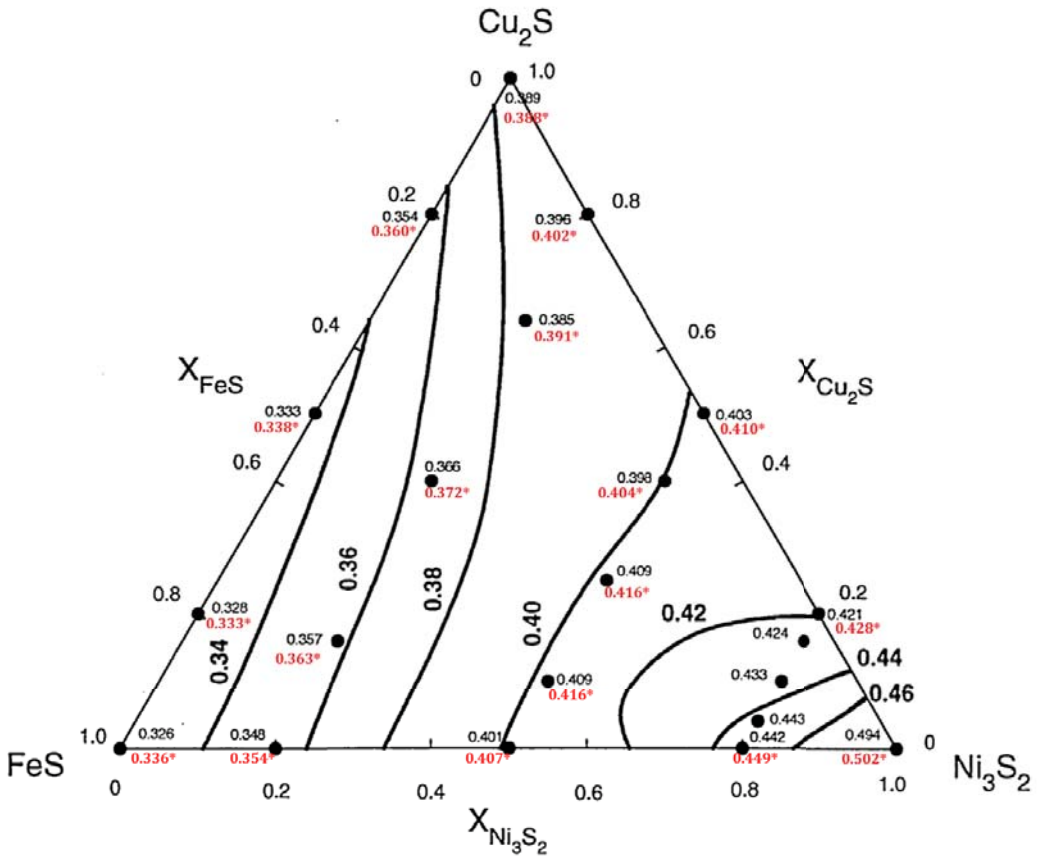

Figure 32: Ternary surface tension diagram for the Cu_2S - Ni_3S_2 - FeS *system at 1200 °C, superimposed on pseudo- ternary system (Kucharski et al., 1993). The experimental points are represented by the closed circles and the solid lines arc iso-tension lines N m* $^{-1}$ *(*Experimental data from this study)*

Figure 32 shows surface tension data for the Cu_2S- Ni_3S_2- FeS pseudo-ternary from this study, superimposed on Kucharski's ternary (Kucharski et al., 1993). As shown in the figure, the experimental data are represented by the closed circles on the ternary diagram while the solid lines are iso-surface tension lines. From Figure 32, it is observed that the surface tension of the matte is sensitive to compositional changes (particularly with changes in the fraction of Ni_3S_2 in the system) for both cases. The ternary diagram also indicates that the addition of Cu_2S to the system does not affect the surface tension significantly. This is reflected by the direction of the iso-surface tension lines which are pointing towards the Cu_2S corner.

4.7 The effect of furnace atmosphere

It has been reported that oxygen of very small amounts leads to the formation of an oxide layer on the droplets and this makes correct contact angle/surface tension measurements difficult (Eustapoulos et al., 1999). Therefore, low oxygen partial pressure environments are desired for surface tension measurements. Sessile drop experiments are performed in inert atmosphere, because of small amounts of oxidizing gas impurities present. In this study, argon gas was employed as an inert atmosphere and was filtered through heated Zr shavings and water using Hydrosorb, keeping the impurities to very low levels where they could not affect the experiment.

An activity of species present during experiments was predicted by calculations which were done in HSC software since the initial conditions are known. Temperatures between 800 ^{o}C and 1300 ^{o}C were considered, Compositions for the three systems in study (*Ni_3S_2*, *Cu_2S*, and *FeS*) and the highest possible amount of oxygen, based on the purity of the Argon gas (0.001 Vol. % oxygen).

The calculated partial pressure of oxygen was found to be in the range -22 and -14 (log) in all cases. (Figures 34 – 39, Appendix IV)

This was regarded as acceptable in preventing any interference from the measurement accuracies. This is also consistent with sulfide smelting operations where P_{O_2} levels are around 10^{-6} to 10^{-8} atm.

For a mixture of gas at low pressure (as in this case), the activity is equal to the ratio of the partial pressure of the gas divided by the standard pressure:

$$a_i = {P_i}/{P^{\Theta}} \qquad \text{Equation 23}$$

Where a_i, is the activity of gaseous species, P_i is the partial pressure of the gas, P^{Θ} is the standard pressure. Since 1 bar = 1 atm, then the activity is equal to the partial pressure for the gaseous species.

As observed in all the results, partial pressure of oxygen in this temperature range (800 °C -1300 °C) is given as:

$$-22 \leq \log P_{O_2} \leq -14 \qquad \text{Equation 24}$$

Even in the Ni_3S_2-Cu_2S (Cu_2S rich) mixture (at 1200 °C) where it was highest, see Table 6; it was within this range. The values are consistent with typical smelting conditions.

Converting partial pressure values (log) into true oxygen partial pressure according to equation:

$$P_{O_2}(atm) = \exp\left(\log P_{O_2}\right) \qquad \text{Equation 25}$$

Table 6 (below) and Table 7 (Appendix IV), shows the true calculated values of partial pressure in atm, in the entire experimental temperature range.

Table 6: Oxygen partial pressure at 1200 °C

System	Po_2 (Log)	Po_2 (atm)
FeS-Ni3S2 (Ni_3S_2 rich)	-21	7.58×10^{-10}
FeS-Ni_3S_2 (*FeS* rich)	-22	2.79×10^{-10}
Cu_2S- *FeS* (Cu_2S rich)	-17	4.14×10^{-8}
Cu_2S- *FeS* (*FeS* rich)	-20	2.06×10^{-9}
Ni_3S_2- Cu_2S (Ni_3S_2 rich)	-13	2.26×10^{-6}
Ni_3S_2- Cu_2S (Cu_2S rich)	-12.5	3.73×10^{-6}

5 Conclusions and Recommendations

5.1 Conclusions

A modified sessile drop method apparatus has been successfully developed to measure surface tension of molten phases resting on substrates. The accuracy of the apparatus has been experimentally demonstrated.

The surface tensions of Ni_3S_2, Cu_2S and FeS molten phases in unary, pseudo-binary and pseudo-ternary system have been experimentally determined using the improved sessile drop technique in the temperature range 1000 – 1300 ^{o}C. The modifications on the optical and temperature measurement system resulted in ease and accuracy for the experiments.

The findings can be summarized as follows:

- The surface tension of the Ni_3S_2 molten phase decreases linearly with increasing temperature in the temperature range of 1000 – 1300 °C. On the other hand, the surface tensions of Cu_2S and FeS molten phases have shown negligible dependency on temperature, i.e. the values remained the same at 386.6 ±5 mNm^{-1} and 339.33±6 mNm^{-1} respectively, in the temperature range 1200 – 1300 $^{\circ}$C.
- For the Ni_3S_2-FeS and Cu_2S-Ni_3S_2 pseudo-binary systems, the surface tensions increased with an increase in Ni_3S_2 content and less so with Cu_2S additions. For Ni_3S_2-FeS, the relationship is linear.
- From the pseudo-ternary measurements, the surface/interfacial tensions of mattes were found to be sensitive to variations in chemical composition of mattes.
- All experimental results were also compared with literature values and were found to be in good agreement with the previous studies. This therefore highlights that the current improved sessile drop method is reliably suitable for carrying out measurements of surface energies of molten mattes.

- Finally, from the findings of this study, a peer reviewed journal article in "Journal of Mineral Processing and Extractive Metallurgy" was published online as given below;

Hamuyuni J., Taskinen P., Akdogan G., Bradshaw S., 2012. Measurement of surface tension of molten matte phases by an improved sessile drop method, *Journal of Mineral Processing and Extractive Metallurgy*, Vol. 121, No. 3, 173 – 177.

5.2 Recommendations

There is a host of factors and properties of molten mattes that are intricately related to surface tensions. Factors such as varying compositions i.e. matte grade of phases involved in smelting, oxygen partial pressure as they relate to surface & interfacial properties of mattes can now be extensively investigated in future with this setup.

The values reported in this study are of fundamental nature for sulfide smelting and they allow interpretations on the phase (gas-slag-matte) separation phenomena in PGM smelting and converting process.

This also opens up opportunities to experimentally study the corrosion of refractory, which has increasingly become a problem in smelters operations.

References

Azuma, K. and Takebe, N., 1972. Densities of molten copper matte. *Nippon Kogyo Kaishi*, vol. 88, pp. 557–562.

Bakker M. L., Nikolic S., and Mackey P. J., 2011. "ISASMELT ™ TSL Applications for Nickel" *Minerals Engineering International, Falmouth*, Minerals Engineering vol. 24, pp. 610–619.

Barfield, R.N. and Kitchener, J.A. 1955. The viscosity of liquid iron and iron-carbon alloys. *Journal of the Iron and Steel Institut*e, vol. 180, pp. 324–329.

Barthel, H., 1981. ‘‘Wear of Chrome Magnesite Bricks in Copper Smelting Furnaces,’’ *Interceram,* vol. 30, pp. 250–255.

Bashforth, F. and Adams, J.C. 1883. An attempt to test the theories of capillary action, Cambridge University Academic Press, London, pp. 1 - 59.

Byerley, J.J. and Takebe, N., 1971. Densities of molten nickel mattes. *Metallurgical Transactions*, vol. 2, no. 4, pp. 1107–1111.

Carla, M., Cecchini, R., 1991. An automated apparatus for interfacial tension measurements by sessile drop technique. Review of Scientific Instruments, vol. 62, pp. 1088 – 1092.

Carlos, D., 1974. Thermodynamic properties of copper-slag systems. INCRA Series on the Metallurgy of Copper. pp. 178.

Chakrabarti, D. J., Laughlin, D. E. 1983. Cu – S (Copper - Sulfur). Binary alloy phase diagrams, ASM, 2nd Edition. Vol. 2, pp. 1467 -1471.

Chiriac, H., Tomut, M., Naum, C., Necula, F., Nagacevschi, V. 1997. On the measurement of surface tension for liquid FeSiB glass-forming alloys by sessile drop method., *Material science and engineering A* vol. 226-228, pp. 341-343.

Chou, K. C., Li, W.-C., Li, F., and He, M. 1996. Formalism of new ternary model expressed in terms of binary regular-solution type parameters, *Calphad*, vol. 20, no. 4, pp. 395–406.

Davenport, W. G., King, M., Schlesinger, M., Biswas, A. K., 2002. Extractive metallurgy of copper, 4 th Edition, Pergamon, pp. 1-71.

Dorsey, N. E. 1928. Measurement of surface tension, Washington academic science 18, pp. 505.

Drelich, J., Fang, C., White, C. L. 2002. Measurement of interfacial tension in fluid-fluid systems, Encyclopedia of Surface and Colloid Science, pp. 3152 - 3166.

Eric R. H., 2004. Slag properties and design issues pertinent to matte smelting electric furnaces, *Southern Africa Institute of Mining and Metallurgy 2004*, pp. 499 – 510.

Eriksson, G. and Pelton, A.D. 1993. Critical evaluation and optimization of the thermodynamic properties and phase diagrams of the calcium-alumina, alumina-silica, and calcium-alumina-silica systems. *Metallurgical and Materials Transactions B*, vol. 24B, pp. 807–816.

Eustathopoulos, N., Nicholas, M. G., Drevet, B. 1999. Wettability at high temperatures 1st edition. Pergamon Materials Series, Oxford, pp. 106-174.

Fagerlund, K. O. and Jalkanen, H., 2000. Microscale simulation of settler process in copper matte smelting, *Metallurgical and Materials Transactions B*, vol. 31, pp. 439-451.

Fujiswa, T. Utigard, T., and Toguri, J.M., 1985. Surface tension and density of the molten lead chloride-potassium chloride-sodium chloride ternary system. *Canadian Journal of Chemistry*, vol. 63, no. 5, pp. 1132–1138.

Fukuyama H., Donald, J. R., and Toguri, J. M., (1997). *Journal of American Ceramic Society,* vol. 80, no.9, pp. 2229–2236.

Harkins, W. D., 1952. The physical chemistry of surface films, Rheinhold, New York, pp. 1 - 413.

Harkins, W.D., Jordan, H.F. 1930. A method for determination of surface and interfacial tension from the maximum pull on a ring. *Journal of American Chemical Society*, vol. 52, pp. 1751–1772.

Heija, A.A. and Eric, R.H., 1997. Aspects of slag optimization in smelting of Cu-Ni sulfide concentrates. Pennsylvania, TMS, pp. 179–192.

Hengzhong, Z., 1993. Relationship between the surface tensions and the compositions of copper and nickel mattes, Paul E. Queneau International *Symposium on Extractive Metallurgy of Copper Nickel and Cobalt*, vol. 1, pp. 341–351.

Hillert, M., 1980. Empirical methods of predicting and representing thermodynamic properties of ternary solution phases, *Calphad*, vol. 4, no. 1, pp. 1–12.

Hryn, J. N., Toguri, J. M., Choo, R. T. C., Stubina, N. M., 1996. Densities of molten copper-nickel mattes between 1100 and 1300 ^{o}C, *Canadian metallurgical quarterly*, Vol. 35, No. 2, pp.123-132.

Imris, I., 2003. Copper losses in copper smelting slags. *Yazawa International Symposium on Metallurgical and Materials Processing: Principles and Technologies*; San Diego, CA; USA; pp. 359-373.

Ip, S. W. and J. M. Toguri, J. M., 1993. ‘‘Interfacial Phenomena in Sulfide Smelting Processes’’ *Extractive Metallurgy of Copper, Nickel and Cobalt, Vol. 1* pp. 289–307.

IP, S. W., Toguri, J. M. 1993. Surface and interfacial tension of the Ni-Fe-S, Ni-Cu-S, and fayalite slag systems, *Metallurgical transaction B* vol. 24B, pp. 657-668.

IP, S. W., Toguri, J. M., 1992. Entrainment behaviour of copper and matte in copper smelting operations, *Metallurgical Transactions B*, vol. 23 B, pp. 303 – 311.

Jing, L., Kexiong, H., Xinmin, C., 1991. Physical phenomena of copper matte smelting, J. CSIMM, Vol. 22, No. 4, pp. 449-455.

Kaiura, G.H. and Toguri, J.M. 1979. Densities of the molten ferrous sulfide, ferrous sulfide-cuprous sulfide and iron-sulfur-oxygen systems—utilizing a bottom-balance Archimedean technique. *Canadian Metallurgical Quarterly*, vol. 18, no. 2, pp. 155–164.

Kaptay, G., 2001. Discussion on "Microscale simulation of settler processes in copper matte smelting", *Metallurgical and Materials Transactions B*, vol. 32, pp. 555-557.

Keene, B.J. 1993. Review of data for surface tension of pure metals, *International Material Reviews* vol. 38, no. 4, pp. 157 – 192.

Kongoli, F. and Pelton, A.D. 1999. Model prediction of thermodynamic properties of Co-Fe-Ni-S mattes. *Metallurgical and Materials Transactions B*, vol. 30B,. pp. 443–450.

Kongoli, F., Dessureault, Y., and Pelton, A.D., 1998. Thermodynamic modeling of liquid Fe-Ni-Cu-Co-S mattes. *Metallurgical and Materials Transactions B*, vol. 29. pp. B:591–601.

Kozakevitch, P., Bockris, J., White, J., Mackenzie, J. 1959. Physicochemical Measurements at High Temperatures, pp.208.

Krivsky, W.A. and Schuhmann, R., 1957. Thermodynamics of the Cu-Fe-S system at matte smelting temperatures, Transactions of the American Institute of Mining and Metallurgy, vol. 209, pp. 981–988.

Kucharski, M., IP, S. W., Toguri, J. M. 1993. The surface tension and density of Cu_2S, Fes, Ni_3S_2 and their mixtures, *Canadian metallurgical quarterly* vol. 33,pp. 197 - 203.

Lecomte du Noüya P, 1919 A new apparatus for measuring surface tension. *Journal of General Physics* vol. 1, pp. 521–524.

Lexow, J., and Bruckner. 1985. Korrosion feuerfester Steine druch fayalitische schemelzen und in Gegenwar von Eisentrofen, Vol. 58, pp. 1-14.

Linchevsky, B., 1979. Methods of metallurgical experiment, *Mir Publishers, Moscow*, pp. 159-180.

Liu, G., Toguri, J.M., and Stubina, N.M. ,1987. Surface tension and density of the molten LaCl3-NaCl binary system. *Canadian Journal of Chemistry*, vol. 65, no. 12. pp. 2779–82.

Liukkonen, M.,1998. Measuring interfacial energy between liquid iron and slag in equilibrium and reaction conditions, Licentiate's thesis, Helsinki University of Technology, *Department of Materials Science and Rock Engineering*, Espoo, pp. 102.

Mäkinen T., Taskinen, P., 2006. The state of the art in nickel smelting, direct outokumpu nickel technology, TMS (*The Minerals, Metals & Materials Society*), pp. 313-325.

Mandira, M., Dharwadkar, H.N., and Kumar, D., 1987. Surface tension of matte and its measurement by sessile drop technique, *Transactions of the Institution of Mining and Metallurgy, Section C: Mineral Processing and Extractive Metallurgy*, vol. 96, pp. C93–C97.

Maru H.C., Wasan D.T., Kintner R.C., 1971. Role of interfacial phenomena in processing metal matrix composite materials. *Chemical Engineering Science* vol. 26, pp. 1615-1628.

Matsushita T., Watanabe T., Hayashi M., and Mukai K., 2011. Thermal, optical and surface & interfacial properties of molten slag systems, *International Materials Reviews*, vol. 56 no. 5-6, pp. 287- 323.

Matsushita, T., Hayashi, M., Seetharaman, S., 2005. Thermochemical and thermo physical property measurements in slag systems, *International Journal of Materials and Product Technology*, vol. 22, no. 4, pp. 351–390.

Minto R., and Davenport W. G., 1972, Entrapment and flotation of matte in molten slag. *Transaction Institute for Mineral processing and Metallurgy* vol. 81C, pp. 36-42.

Mukai K., 1985. Recent studies on the interfacial phenomena in which Marangoni effect participates, Testu-tu-Hagane, vol. 71, pp.1435-1440.

Mukai K., 1998. Marangoni flows and corrosion of refractory walls. *Philosophical Transactions of the Royal Society London A*, vol. 356A, pp. 1015–1026.

Mukai K., Toguri J., Kodama, M. I., and Yoshitomi J.,1986. Effect of Applied Potential on the Interfacial Tension between Liquid Lead and $PbO.SiO_2$ Slags. Canadian Metallurgical Quarterly vol. 25, pp. 225–231.

Mukai, K., 1992. Wetting and Marangoni Effect in Iron and Steelmaking Processes, *The Iron and Steel Institute of Japan*, Vol. 32, no. 1, pp. 19-25.

Nagamori, M. 1969. Density of molten Ag-S, Cu-S, FeS, and Ni-S systems, *Transactions of the metallurgical society of AIME* vol. 245, pp. 1897 - 1902.

Nakamoto, M., Liukkonen, M., Freeman, M., Heikinhemo, E., Hämäläinen, M., Holappa, L. 2008. Measurement of surface tension of solid Cu by improved

multiphase equilibrium, Metallurgical *and materials transaction B,* Vol. 39B, pp. 570 – 580.

Nakamura T., Toguri J. M., 1991. Interfacial phenomena in copper smelting processes, *In Copper 91-Cobre 91 Proceedings of the Second International Conference,* Vol. IV Pyrometallurgy of Copper, ed. Diaz, C., Landolt, C., Luraschi, A.A. and Newman, C.J., Pergamon Press, New York, NY, pp. 537 551.

Nakamura T., Yokoyama K., Noguchi F., and Mukai K., 1991. Direct Observations of Marangoni Convection in Molten Salts, *Material Science Forum,* vol. 73–75, pp. 153–158.

Nikiforov, L.V., Nagiev, V.A., and Grabchak, V.P., 1976. Viscosity of sulfide melts. Izvestiya Akademii Nauk SSSR, *Neorganicheskie Materialy*, vol. 12, no. 7, pp. 1179–1182.

Outotec; (01.01.2012), Outotec flash smelting and kennecott-outotec flash converting process flow sheet.

Pelton, A.D. and Blander, M. 1986. Thermodynamic analysis of ordered liquid solutions by a modified quasi chemical approach-application to silicate slags. *Metallurgical and Materials Transactions B*, vol. 17B, pp. 805–815.

Poggi D., Minto R., Davenport W. G., 1969. Mechanisms of metal entrapment in slags, *Journal of Metals*, vol. 21,pp. 40-45.

Rigby A. J, 1993. ‘‘Wear Mechanisms of Refractory Linings of Converters and Anode Furnaces’’ *Converting, Fire Refining and Casting,* pp. 155–68.

Sahoo P., Debroy T., and McNallan M. J., 1988. Surface tension of binary metal-surface active solute systems under conditions relevant to welding metallurgy, *Metallurgical and Materials Transactions B*, vol. 19, no. 3, pp. 483-491.

Seetharaman S., 2005. Fundamentals of Metallurgy, *Woodhead publishing Limited,* London, pp. 38 – 81.

Sergin, B. I., Lepinskikh, B. M. 1964. Tr. Pervoi. Sverdl. Nauchu-Tekhn. Konf. Molodykh Uchenykh, Akad. Nauk. SSSR, Ural’sk. Filial*. Inst. Met., Sverdlovsk Pt* I, pp 9-11.

Singleton, M., Nash, P., Lee, K.J. 1991. Ni – S (Nickel Sulfur). Binary alloy phase diagrams, ASM, 2nd Edition. vol. 3, pp. 2850 – 2853.

Sugden S., 1922. The determination of surface tension from the maximum pressure in bubbles *Journal of Chemical Society Transaction.*, pp. 121, 858

Sundström, A.W., Eksteen, J.J., Georgalli, J. J., 2008. A review of the physical properties of base metal mattes, *Journal of Southern Africa institute of Mining and Metallurgy*, vol. 108, pp. 431-448.

Tarek El Gammal, I. The significance of interfacial phenomena in the metallurgical processes. Institute of Ferrous Metallurgy. Aachen University of Technology. Available at; http://www.ariel.ac.il/management/research/pf/zinigrad/mmt/MMT-2000/papers/547-557.doc

Thiessen, D. B. and Man, K. F., 1999. The Measurement, Instrumentation, and Sensor Handbook, J. G. Webster, ed. (CRC Press and IEEE Press, Boca Raton, FL, 1999), (Chapter 31)pp. 1-13.

Tiida, T., Guthrie, R. I., 1988. Physical properties of liquid metals, Oxford University press, pp. 109-146.

Tokumoto, S., Kasama, A., Fujioka, Y. 1972. Measurements of density and surface tension of copper mattes, Technology reports of the Osaka University vol. 22, pp.453 - 463.

Turkdogan, E. T., 1980. Physical chemistry of high temperature technology, *Academic Press*, pp. 92-129.

Vaarno, J., Jarvi, J., Ahokainen, T. & Laurila, T., Taskinen, P., 2003. Development of a mathematical model of flash smelting and converting process. 3rd international conference on CFD in the minerals and process industries, CSIRO, Melborn, Australia. pp. 147-154.

Vanyukov, A.V., Bytrov, V.P., Zaytsev, V., 1966. Surface and interfacial tension of lead-bearing metallurgical melts. *Eizicheskaya Khimiya Metallurgicheskih Protsessov I Sistem*, pp. 396–406

VISION SYSTEMS., VISI50 Available online (October 2012).

Waldner, P. and Pelton, A.D., 2004. Critical thermodynamic assessment and modelling of the Fe-Ni-S system. *Metallurgical and Materials Transactions B*, vol. 35B,. pp. 897–907.

Waldner, P., Pelton, A. D. 2005. Thermodynamic modeling of the FeS system, Journal of Phase Equilibria and Diffusion Vol. 26 no.1, pp. 23 – 38.

Wernick I., Themelis, N.J., 1998. Recycling Metals for the Environment, *Annual Reviews Energy and Environment*, vol. 23, pp. 465-97.

White, D. WG. 1967. A supplement to the Tables of Bashforth and Adams, *Transaction of American Society of Metallurgy, pp.* 55, 757.

White, H. E., Modern College Physics, 4 Th Edition, New York, (1948).

WU, P., Eriksson, G., and Pelton, A.D. 1993. Critical evaluation and optimization of the thermodynamic properties and phase diagrams of the calcia-iron(II) oxide, calcia-magnesia, calcia-manganese(II) oxide, iron(II) oxidemagnesia, iron(II) oxide manganese(II) oxide, and magnesiamanganese(II) oxide systems. *Journal of the American Ceramic Society*, vol. 76. pp. 2059–2064.

Yan, L., Cao, Z., Xie, Y., and Qiao, Z., 2000. Surface tension calculation of the Ni3S2-FeS-Cu2S mattes, *Calphad*, vol. 24, no. 4, pp. 449–463.

Zaytsev, V. Ya., Vanyukov, A. V., Kolosova 1968. Isv. Akad. Nauk SSSR, Metal., No. 5, pp. 39-41.

Appendix I: Typical values from the Bashforth and Adams Tables

	β									
	1.5		2.0		2.5		3.0		3.5	
ϕ	$\frac{x}{b}$	$\frac{z}{b}$	$\frac{x}{b}$	$\frac{z}{b}$	$\frac{x}{b}$	$\frac{z}{b}$	$\frac{x}{b}$	$\frac{z}{b}$	$\frac{x}{b}$	$\frac{z}{b}$
5	.08703	.00380	0.8699	.00379	.08695	.00379	.08691	.00379	.08687	.00379
10	.17268	.01507	.17236	.01502	.17204	.01498	.17173	.01494	.17142	.01490
15	.25564	.03344	.25462	.03324	.25363	.03305	.25265	.03286	.25170	.03268
20	.33479	.05838	.33255	.05779	.33039	.05723	.32830	.05668	.32628	.05615
25	.40923	.08920	.40523	.08787	.40143	.08662	.39780	.08543	.39434	.08430
30	.47826	.12511	.47203	.12262	.46619	.12030	.46071	.11814	.45553	.11613
35	.54144	.16533	.53260	.16117	.52446	.15739	.51691	.15391	.50988	.15071
40	.59848	.20908	.58681	.20274	.57621	.19707	.56651	.19194	.55756	.18726
45	.64928	.25560	.63469	.24658	.62161	.23863	.60978	.23155	.59898	.22517
50	.69385	.30420	.67636	.29203	.66089	.28146	.64703	.27216	.63448	.26387
55	.73229	.35427	.71206	.33851	.69435	.32503	.67862	.31330	.66448	.30294
60	.76478	.40522	.74203	.38552	.72231	.36888	.70492	.35454	.68939	.34199
65	.79152	.45655	.76656	.43261	.74510	.41262	.72629	.39556	.70956	.38073
70	.81277	.50780	.78596	.47939	.76305	.45592	.74308	.43604	.72539	.41886
75	.82879	.55857	.80052	.52552	.77649	.49847	.75561	.47573	.73718	.45622
80	.83987	..60850	.81055	.57070	.78572	.54004	.76420	.51442	.74523	.49255
85	.84630	.65724	.81635	.61466	.79104	.58038	.76915	.55191	.74989	.52771
90	.84838	.70453	.81822	.65717	.79275	.61931	.77074	.58803	.75137	.56154
95	.84640	.75009	.81645	.69802	.79113	.65665	.76924	.62262	.74998	.59391
100	.84067	.79371	.81133	.73702	.78646	.69224	.76491	.65556	.74593	.62472
105	.83150	.83516	.80314	.77401	.77899	.72596	.75801	.68674	.73948	.65386
110	.81917	.87427	.79216	.80886	.76900	.75768	.74878	.71605	.73086	.68122
115	.80402	.91089	.77868	.84143	.75674	.78730	.73745	.74340	.72027	.70674
120	.78634	.94487	.76297	.87162	.74246	.81474	.72428	.76873	.70799	.73039
125	.76644	.97612	.74531	.89935	.72642	.83994	.70948	.79198	.69417	.75209
130	.74465	1.00453	.72598	.92456	.70886	.86283	.69328	.81310	.67906	.77182
135	.72128	1.03006	.70525	.94720	.69004	.88339	.67590	.83207	.66284	.78949
140	.69663	1.05264	.68339	.96723	.67018	.90159	.65758	.84887	.64574	.80519
145	.67105	1.07229	.66068	.98467	.64954	.91744	.63851	.86350	.62792	.81884
150	.64482	1.08901	.63738	.99952	.62834	.93095	.61893	.87599	.60963	.83050
155	.61826	1.10284	.61375	1.01183	.60681	.94217	.59901	.88636	.59101	.84020
160	.59167	1.11387	.59003	1.02166	.58518	.95113	.57898	.89467	.57223	.84798
165	.56532	1.12218	.56647	1.02910	.56364	.95793	.55901	.90097	.55353	.85390
170	.53949	1.12792	.54329	1.03425	.54240	.96265	.53927	.90535	.53500	.85802
175	.51439	1.13123	.52069	1.03723	.52164	.96538	.51994	.90790	.51684	.86041
180	.49026	1.13229	.49885	1.03819	.50151	.96630	.50116	.90872	.50914	.86117

N. B. The values in the table above are an extract from the Mercury drop shape calculations, adapted from Bashforth and Adams, 1983

Appendix II: Acknowledgments – Aalto University

Aalto University of Espoo (Finland) and Stellenbosch University have been collaborating since 2009 in various fields of metals extraction. This cooperation includes exchange of scientists and experience in joint research projects of Professors Guven Akdogan and Pekka Taskinen, dealing with several hydro and pyrometallurgical operations in non-ferrous metal making as well as fundamental principles of equilibrium and transport phenomena related to them. An important feature of such long term scientific cooperation is mobility of scientists, in order to transfer knowledge and skills in core areas of science and engineering. Mr. Joseph Hamuyuni has been a member of the Thermodynamics and Modeling research group of Aalto University, School of Chemical Technology and its Department of Materials Science and Engineering since August 2011, within the framework of this joint effort. He has studied the surface properties of molten metal sulfides at elevated temperatures. They are the basic building blocks of industrial sulfide mattes used in copper, nickel and precious metals (PGM) extraction. He has utilized the advanced sessile drop apparatus, developed at the Department of Aalto University. It has been recently updated with a HD digital camera system for drop profile measurements with improved accuracy, *in situ* at elevated temperatures, for evaluating the surface energies of the molten sulfides and their mixtures as a function of temperature and composition. The values are of fundamental nature in sulfide smelting and allow later estimations about phase (gas-slag-matte) separation phenomena, i.e. in PGM smelting and converting process.

The author would like to thank Prof. Guven Akdogan and Prof. S.M. Bradshaw, for the tremendous support and supervision of this work. Many thanks also to Stellenbosch OSP Fund, for financial support to this project.

Appendix III: Images in sequence illustrating profiles of melting Sulfides

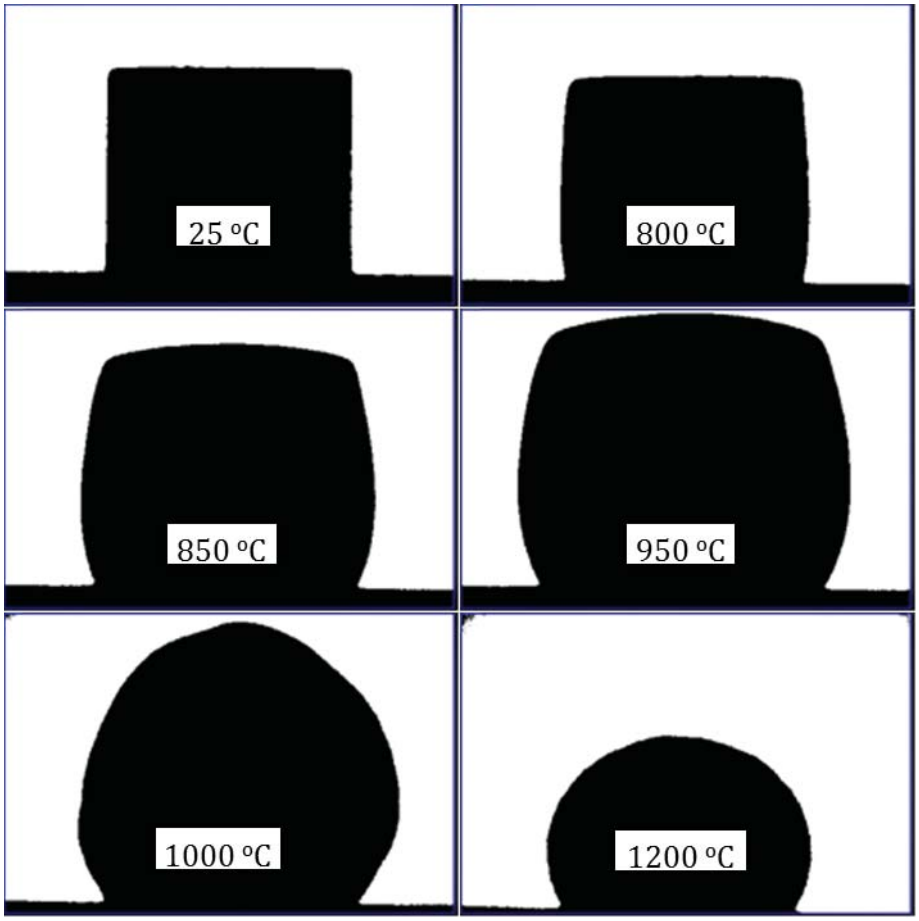

Figure 33: Binary images of sulfide melt at different temperatures

Appendix IV: Profiles of activity for different compositions (mol. %)

The graphs in Figure 34 - 39 shows activity (log) of various pure species of pure substances as a function of temperature (°C). Oxygen (O_2) which is of great interest is among the species.

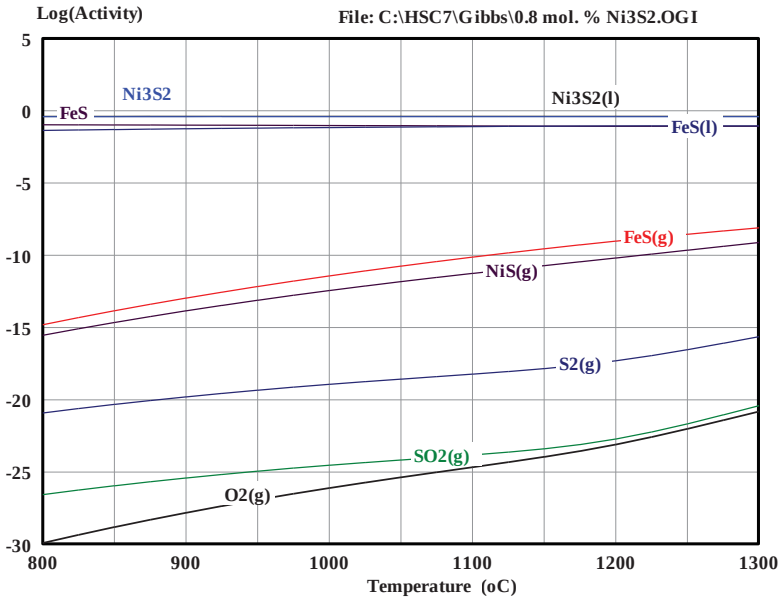

Figure 34: Activity in the FeS-Ni_3S_2 mixture (Ni_3S_2 rich)

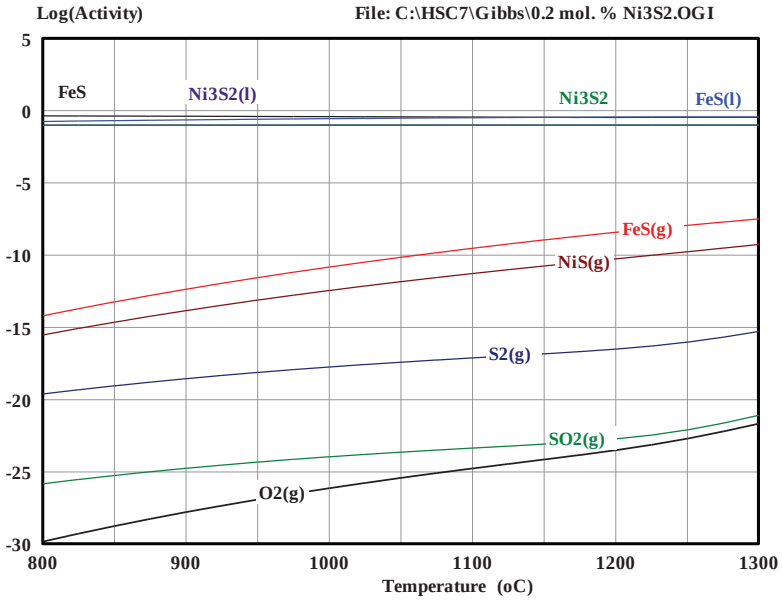

Figure 35: Activity in the FeS-Ni_3S_2 mixture (FeS rich)

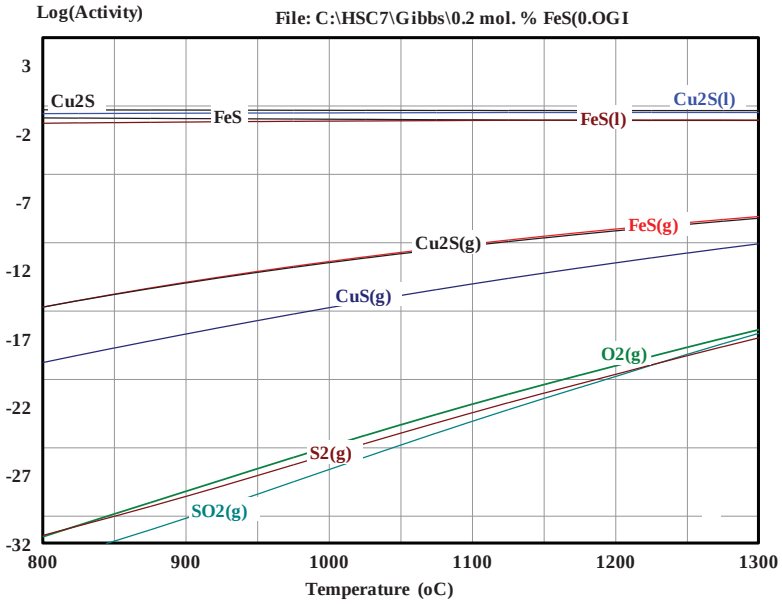

Figure 36: Activity in the Cu_2S-FeS mixture (Cu_2S rich)

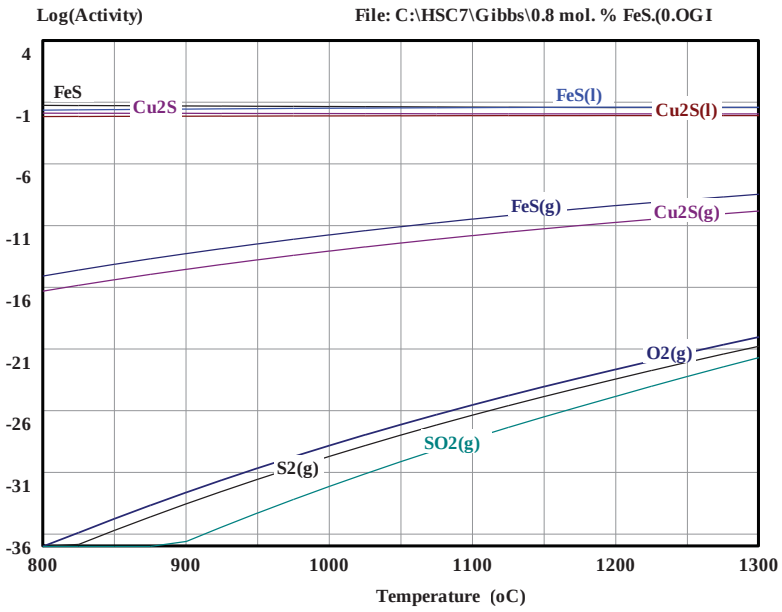

Figure 37: Activity in the Cu_2S-FeS mixture (FeS rich)

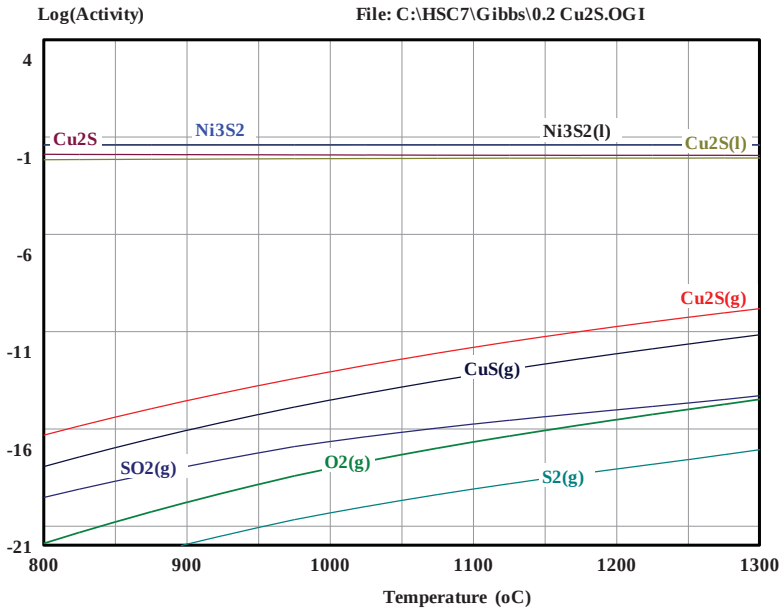

Figure 38: Activity in the Cu_2S-Ni_3S_2 mixture (Ni_3S_2 rich)

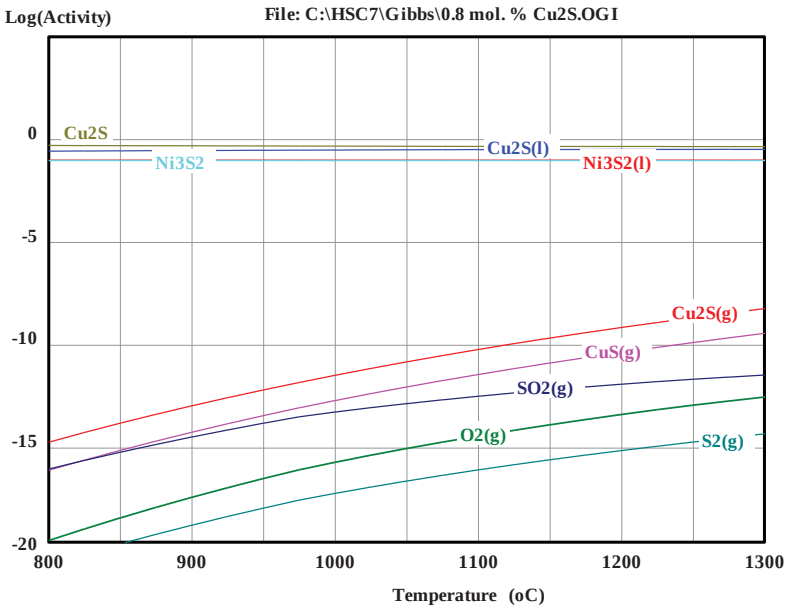

Figure 39: Activity in the Cu_2S-Ni_3S_2 mixture (Cu_2S rich)

Table 7: Oxygen partial pressure at 800 °C, 1000 °C, and 1300 °C

System	800 °C		1000 °C		1300 °C	
	Log (Po_2)	**PO_2 (atm)**	**Log (Po_2)**	**PO_2 (atm)**	**Log (Po_2)**	**PO_2 (atm)**
FeS-Ni_3S_2 (*Ni_3S_2* rich)	-30	9.36×10^{-14}	-24	3.78×10^{-11}	-22	2.79×10^{-10}
FeS-Ni_3S_2 (*FeS* rich)	-30	9.36×10^{-14}	-26	5.11×10^{-12}	-22	2.79×10^{-10}
Cu_2S- FeS (*Cu_2S* rich)	-31	3.44×10^{-14}	-26	5.11×10^{-12}	-16	1.13×10^{-7}
Cu_2S- FeS (*FeS* rich)	-36	2.32×10^{-16}	-28	6.91×10^{-13}	-19	5.6×10^{-9}
Ni_3S_2- Cu_2S (*Ni_3S_2* rich)	-21	7.58×10^{-10}	-17	4.14×10^{-8}	-14	8.32×10^{-7}
Ni_3S_2- Cu_2S (*Cu_2S* rich)	-20	2.06×10^{-9}	-14	8.32×10^{-7}	-12,5	3.73×10^{-6}

Appendix V: Table of results of surface tension

Ni_3S_2					Cu_2S				FeS		
1000 °C	**1100 °C**	**1200 °C**	**1300 °C**		**1200 °C**	**1250 °C**	**1300 °C**		**1200 °C**	**1250 °C**	**1300 °C**
536.5	515.5	501.53	452.82		388.29	390.0	381.5		335.60	345.80	336.60
536.5	515.5	501.53	452.82		401.01	390.0	381.5		335.60	345.80	336.60
536.5	515.5	501.53	452.82		388.29	390.0	381.5		335.60	345.80	336.60
536,5	515.5	501.53	452.82		388.29	390.0	381.5		335.60	345.80	303.42
536.5	515.5	501.53	452.82		388.29	390.0	324.4		335.60	345.80	336.60
536.5	515.5	478.54	452.82		388.29	390.0	381.5		285.19	345.80	336.60
536.5	515.5	501.53	452.82		388.29	390.0	381.5		335.60	345.80	336.60
536.5	515.5	501.53	452.82		388.29	390.0	381.5		335.60	345.80	336.60
536.5	515.5	501.53	452.82		388.29	390.0	381.5		335.60	345.80	336.60
536.5	515.5	501.53	452.82		337.79	390.0	381.5		335.60	307.19	336.60
536.5	515.5	501.53	452.82		388.29	390.0	445.2		335.60	345.80	336.60
536.5	491.9	501.53	452.82		388.29	390.0	381.5		335.60	345.80	336.60
536.5	515.5	501.53	452.82		388.29	314.4	381.5		335.60	345.80	336.60
536.5	515.5	501.53	452.82		388.29	390.0	381.5		335.60	345.80	336.60
536.5	515.5	501.53	452.82		388.29	390.0	381.5		335.60	345.80	336.60

From the table, the values are surface tension values (mNm^{-1}) at various given temperatures